Estimating the burden of SARS-CoV-2 in France

Henrik Salje, Cécile Tran Kiem, Noémie Lefrancq, Noémie Courtejoie, Paolo Bosetti, Juliette Paireau, Alessio Andronico, Nathanaël Hoze, Jehanne Richet, Claire-Lise Dubost, et al.

Estimating the burden of SARS-CoV-2 in France

Henrik Salje, Cécile Tran Kiem, Noémie Lefrancq, Noémie Courtejoie, Paolo Bosetti, Juliette Paireau, Alessio Andronico, Nathanaël Hozé, Jehanne Richet, Claire-Lise Dubost, et al.

Estimating the burden of SARS-CoV-2 in France

Henrik Salje[1,2,3*], Cécile Tran Kiem,[1,4,*], Noémie Lefrancq[1], Noémie Courtejoie[5], Paolo Bosetti[1], Juliette Paireau[1,6], Alessio Andronico[1], Nathanaël Hozé[1], Jehanne Richet[5], Claire-Lise Dubost[5], Yann Le Strat[6], Justin Lessler[3], Daniel Levy Bruhl[6], Arnaud Fontanet[7,8], Lulla Opatowski[9,10], Pierre-Yves Boelle[11], Simon Cauchemez[1]

1. Mathematical Modelling of Infectious Diseases Unit, Institut Pasteur, UMR2000, CNRS, France
2. Department of Genetics, University of Cambridge, Cambridge, UK
3. Department of Epidemiology, Johns Hopkins Bloomberg School of Public Health, Baltimore, Maryland, USA
4. Collège Doctoral, Sorbonne Université, Paris, France
5. DREES, Ministère des Solidarités et de la Santé, Paris, France
6. Santé Publique France, French National Public Health Agency, Saint-Maurice, France
7. Emerging Diseases Epidemiology Unit, Institut Pasteur, Paris, France
8. PACRI Unit, Conservatoire National des Arts et Métiers, Paris, France
9. Epidemiology and Modelling of Antibiotic Evasion Unit, Institut Pasteur, Paris, France
10. Anti-infective evasion and pharmacoepidemiology team, CESP, Université Paris-Saclay, UVSQ, INSERM U1018, Montigny-le-Bretonneux, France.
11. Institut Pierre Louis d'Epidémiologie et de Santé Publique, Sorbonne Université, INSERM,Paris, France

*These authors contributed equally to the work

Correspondence to:
Simon Cauchemez
Mathematical Modelling of Infectious Diseases Unit
Institut Pasteur
28 rue du Dr Roux
Paris 75015
simon.cauchemez@pasteur.fr

Abstract

France has been heavily affected by the SARS-CoV-2 epidemic and went into lockdown on the 17th March 2020. Using models applied to hospital and death data, we estimate the impact of the lockdown and current population immunity. We find 3.6% of infected individuals are hospitalized and 0.7% die, ranging from 0.001% in those <20 years of age (ya) to 10.1% in those >80ya. Across all ages, men are more likely to be hospitalized, enter intensive care, and die than women. The lockdown reduced the reproductive number from 2.90 to 0.67 (77% reduction). By 11 May 2020, when interventions are scheduled to be eased, we project 2.8 million (range: 1.8-4.7) people, or 4.4% (range: 2.8 - 7.2) of the population, will have been infected. Population immunity appears insufficient to avoid a second wave if all control measures are released at the end of the lockdown.

Main

The worldwide pandemic of SARS-CoV-2, the coronavirus which causes COVID-19, has resulted in unprecedented responses, with many affected nations confining residents to their homes. Much like the rest of Europe, France has been hit hard by the epidemic and went into lockdown on the 17th March 2020. It was hoped that this would result in a sharp decline in ongoing spread, as was observed when China locked down following the initial emergence of the virus (*1*, *2*). Following the expected reduction in cases, the French government has announced it will ease restrictions on the 11th May 2020. To exit from the lockdown without escalating infections, we need to understand the underlying level of population immunity and infection, identify those most at risk for severe disease and the impact of current control efforts.

Daily reported numbers of hospitalizations and deaths only provide limited insight into the state of the epidemic. Many people will either develop no symptoms or symptoms so mild they will not be detected through healthcare-based surveillance. The concentration of hospitalized cases in older individuals has led to hypotheses that there may be widespread 'silent' transmission in younger individuals (*3*). If the majority of the population is infected, viral transmission would slow, potentially reducing the need for the stringent intervention measures currently employed.

We present a suite of modelling analyses to characterize the dynamics of SARS-CoV-2 transmission in France and the impact of the lockdown on these dynamics. We elucidate the risk of SARS-CoV-2 infection and severe outcomes by age and sex and estimate the current proportion of the national and regional populations that have been infected and might be at least temporarily immune (*4*). These models support healthcare planning of the French government by capturing hospital bed capacity requirements.

As of 7 May 2020, there were 95,210 incident hospitalizations due to SARS-CoV-2 reported in France and 16,386 deaths in hospitals, with the east of the country and the capital, Paris, particularly affected (Figure 1A-B). The mean age of hospitalized patients was 68ya and the mean age of the deceased was 79ya with 50.0% of hospitalizations occurring in individuals >70ya and 81.6% of deaths within that age bracket; 56.2% of hospitalizations and 60.3% of deaths were male (Figures 1C-E). To reconstruct the dynamics of all infections, including mild ones, we jointly analyze French hospital data with the results of a detailed outbreak investigation aboard the Diamond Princess cruise ship where all passengers were subsequently tested (719 infections, 14 deaths currently). By coupling the passive surveillance data from French hospitals with the active surveillance performed aboard the Diamond Princess, we disentangle the risk of being hospitalized in those infected from the underlying probability of infection (*5*, *6*).

We find that 3.6% of infected individuals are hospitalized (95% CrI: 2.1-5.6), ranging from 0.2% (95% CrI: 0.1-0.2) in females under <20ya to 45.9% (95% CrI: 27.2-70.9) in males >80ya (Figure 2A, Table S1). Once hospitalized, on average 19.0% (95% CrI: 18.7%-19.4%) patients enter ICU after a mean delay of 1.5 days (Figure S1). We observe an increasing probability of entering ICU with age - however, this drops for those >70ya (Figure 2B, Table S2). Overall, 18.1% (95% CrI: 17.8-18.4) of hospitalized individuals go on to die (Figure 2C). The overall probability of death

among those infected (the Infection Fatality Ratio, IFR) is 0.7% (95% CrI: 0.4-1.0), ranging from 0.001% in those under 20ya to 10.1% (95% CrI: 6.0-15.6) in those >80ya (Figure 2D, Table S2). Our estimate of overall IFR is similar to other recent studies that found values of between 0.5%-0.7% for the Chinese epidemic (*6*–*8*). We find men have a consistently higher risk than women of hospitalization (RR 1.25, 95% CrI: 1.22-1.29), ICU admission once hospitalized (RR: 1.61, 95% CrI: 1.56-1.67) and death following hospitalization (RR: 1.47, 95% CrI: 1.42-1.53) (Figure S2).

We identify two clear subpopulations in those cases that are hospitalized: individuals that die quickly upon hospital admission (15% of fatal cases, mean time to death of 0.67 days) and individuals who die after longer time periods (85% of fatal cases, mean time to death of 13.2 days) (Figure S3). The proportion of fatal cases who die rapidly remains approximately constant across age-groups (Figure S4, Table S3). Potential explanations for different subgroups of fatal cases include heterogeneous patterns of healthcare seeking, access to care, underlying comorbidities, such as metabolic disease and other inflammatory conditions. A role for immunopathogenesis has also been proposed (*9*–*12*).

We next fit national and regional transmission models to ICU admission, hospital admission, and bed occupancy (both ICU and general wards) (Figure 3A-D, Figure S5, Tables S4-S6), allowing for reduced age-specific daily contact patterns following the lockdown and changing patterns of ICU admission over time (Figure S17). We find that the basic reproductive number R_0 prior to the implementation of the lockdown was 2.90 (95% CrI: 2.80-2.99). The lockdown resulted in a 77% (95%CI: 76-78) reduction in transmission, with the reproduction number R dropping to 0.67 (95% CrI: 0.65-0.68). We forecast that by the 11th May 2020, 2.8 million (range 1.8 - 4.7, when accounting for uncertainty in the probability of hospitalization given infection) people will have been infected, representing 4.4% (range 2.8 - 7.2) of the French population (Figure 3E). This proportion will be 9.9% (range 6.6-15.7) in Ile-de-France, which includes Paris, and 9.1% (range 6.0-14.6) in Grand Est, the two most affected regions of the country (Figure 3F, Figure S5). Assuming a basic reproductive number of R_0=3.0, it would require around 65% of the population to be immune for the epidemic to be controlled by immunity alone. Our results therefore strongly suggest that, without a vaccine, herd immunity on its own will be insufficient to avoid a second wave at the end of the lockdown. Efficient control measures need to be maintained beyond the 11th May.

Our model can help inform the ongoing and future response to COVID-19. National ICU daily admissions have gone from 700 at the end of March to 66 on the 7th May., Hospital admissions have declined from 3600 to 357 over the same time period, with consistent declines observed throughout France (Figure S5). By the 11th May we project 3900 (range: 2600 - 6300) daily infections across the country, down from between 150,000-390,000 immediately prior to the lockdown. At a regional level, we estimate that 58% of infections will be in Ile-de-France and Grand Est combined. We find that the time people spend in ICU appears to differ across the country, which may be due to differences in health care practises (Table S5).

Using our modelling framework, we are able to reproduce the observed number of hospitalizations by age and sex in France and the number of observed deaths aboard the Diamond Princess

(Figure S6). As a validation, our approach is also able to correctly identify parameters in simulated datasets where the true values are known (Figure S7). As cruise ship passengers may represent a different, healthier population than average French citizens, we run a sensitivity analysis where Diamond Princess passengers are 25% less likely to die than French citizens (Figure 4, Figure S8). We also run sensitivity analyses with longer delays between symptom onset and hospital admission, missed infections aboard the Diamond Princess, equal attack rates across all ages, reduced infectivity in younger individuals, a contact matrix with unchanged structure before/during the lockdown and one with very high isolation of elderly individuals during the lockdown. These different scenarios result in mean IFRs from 0.5% to 0.9%, the proportion of the population infected by the 11 May 2020 ranging from 1.7%-8.9%, the number of daily infections at this date ranging from 1700-9600 and a range of reproductive numbers post lockdown of 0.62-0.73 (Figure 4, Figures S8-S15, Table S7-S12).

A seroprevalence of 3% (range 0-3%) has been estimated among blood donors in Hauts-de-France, which is consistent with our model predictions (range: 1%-3%) for this population if we account for a 10-day delay for seroconversion (*13*, *14*). Future additional serological data will help further refine estimates of the proportion of the population infected.

While we focus on deaths occurring in hospitals, there are also non-hospitalized COVID-19 deaths, including >9,000 in retirement homes in France (*15*). We explicitly removed retirement home population from our analyses as transmission dynamics may be different in these closed populations. This means our estimates of immunity in the general population are unaffected by deaths in retirement homes, however, in the event of large numbers of non-hospitalized deaths in the wider community, we would underestimate the proportion of the population infected. Analyses of excess death will be important to explore these issues.

This study shows the massive impact the French lockdown had on SARS-CoV-2 transmission. Our modelling approach has allowed us to estimate underlying probabilities of infection, hospitalization and death, which is essential for the interpretation of COVID-19 surveillance data. The forecasts we provide can inform lockdown exit strategies. Our estimates of a low level of immunity against SARS-CoV-2 indicates that efficient control measures that limit transmission risk will have to be maintained beyond the 11th May 2020 to avoid a rebound of the epidemic.

References

1. M. U. G. Kraemer, C.-H. Yang, B. Gutierrez, C.-H. Wu, B. Klein, D. M. Pigott, Open COVID-19 Data Working Group, L. du Plessis, N. R. Faria, R. Li, W. P. Hanage, J. S. Brownstein, M. Layan, A. Vespignani, H. Tian, C. Dye, O. G. Pybus, S. V. Scarpino, The effect of human mobility and control measures on the COVID-19 epidemic in China. *Science* (2020), doi:10.1126/science.abb4218.

2. H. Tian, Y. Liu, Y. Li, C.-H. Wu, B. Chen, M. U. G. Kraemer, B. Li, J. Cai, B. Xu, Q. Yang, B. Wang, P. Yang, Y. Cui, Y. Song, P. Zheng, Q. Wang, O. N. Bjornstad, R. Yang, B. T. Grenfell, O. G. Pybus, C. Dye, An investigation of transmission control measures during the first 50 days of the COVID-19 epidemic in China. *Science* (2020), doi:10.1126/science.abb6105.

3. J. Lourenço, R. Paton, M. Ghafari, M. Kraemer, C. Thompson, P. Simmonds, P. Klenerman, S. Gupta, Fundamental principles of epidemic spread highlight the immediate need for large-scale serological surveys to assess the stage of the SARS-CoV-2 epidemic. *medRxiv* (2020) (available at https://www.medrxiv.org/content/10.1101/2020.03.24.20042291v1.abstract).

4. L. Bao, W. Deng, H. Gao, C. Xiao, J. Liu, J. Xue, Q. Lv, J. Liu, P. Yu, Y. Xu, F. Qi, Y. Qu, F. Li, Z. Xiang, H. Yu, S. Gong, M. Liu, G. Wang, S. Wang, Z. Song, W. Zhao, Y. Han, L. Zhao, X. Liu, Q. Wei, C. Qin, Reinfection could not occur in SARS-CoV-2 infected rhesus macaques. *bioRxiv*, , doi:10.1101/2020.03.13.990226.

5. J. Lessler, H. Salje, M. D. Van Kerkhove, N. M. Ferguson, S. Cauchemez, I. Rodriquez-Barraquer, R. Hakeem, T. Jombart, R. Aguas, A. Al-Barrak, D. A. T. Cummings, MERS-CoV Scenario and Modeling Working Group, Estimating the Severity and Subclinical Burden of Middle East Respiratory Syndrome Coronavirus Infection in the Kingdom of Saudi Arabia. *Am. J. Epidemiol.* **183**, 657–663 (2016).

6. R. Verity, L. C. Okell, I. Dorigatti, P. Winskill, C. Whittaker, N. Imai, G. Cuomo-Dannenburg, H. Thompson, P. G. T. Walker, H. Fu, A. Dighe, J. T. Griffin, M. Baguelin, S. Bhatia, A. Boonyasiri, A. Cori, Z. Cucunubá, R. FitzJohn, K. Gaythorpe, W. Green, A. Hamlet, W. Hinsley, D. Laydon, G. Nedjati-Gilani, S. Riley, S. van Elsland, E. Volz, H. Wang, Y. Wang, X. Xi, C. A. Donnelly, A. C. Ghani, N. M. Ferguson, Estimates of the severity of coronavirus disease 2019: a model-based analysis. *Lancet Infect. Dis.* (2020), doi:10.1016/S1473-3099(20)30243-7.

7. T. W. Russell, J. Hellewell, C. I. Jarvis, K. van Zandvoort, S. Abbott, R. Ratnayake, Cmmid Covid-Working Group, S. Flasche, R. M. Eggo, W. J. Edmunds, A. J. Kucharski, Estimating the infection and case fatality ratio for coronavirus disease (COVID-19) using age-adjusted data from the outbreak on the Diamond Princess cruise ship, February 2020. *Euro Surveill.* **25** (2020), doi:10.2807/1560-7917.ES.2020.25.12.2000256.

8. K. Mizumoto, K. Kagaya, G. Chowell, Early epidemiological assessment of the transmission potential and virulence of coronavirus disease 2019 (COVID-19) in Wuhan City: China, January-February, 2020. *medRxiv* (2020) (available at https://www.medrxiv.org/content/10.1101/2020.02.12.20022434v2.abstract).

9. L. Peeples, News Feature: Avoiding pitfalls in the pursuit of a COVID-19 vaccine. *Proc. Natl. Acad. Sci. U. S. A.* (2020), doi:10.1073/pnas.2005456117.

10. D. Ricke, R. W. Malone, Medical Countermeasures Analysis of 2019-nCoV and Vaccine

Risks for Antibody-Dependent Enhancement (ADE) (2020), , doi:10.2139/ssrn.3546070.

11. J. Yang, Y. Zheng, X. Gou, K. Pu, Z. Chen, Q. Guo, R. Ji, H. Wang, Y. Wang, Y. Zhou, Prevalence of comorbidities and its effects in patients infected with SARS-CoV-2: a systematic review and meta-analysis. *International Journal of Infectious Diseases*. **94** (2020), pp. 91–95.

12. M. Bolles, D. Deming, K. Long, S. Agnihothram, A. Whitmore, M. Ferris, W. Funkhouser, L. Gralinski, A. Totura, M. Heise, R. S. Baric, A Double-Inactivated Severe Acute Respiratory Syndrome Coronavirus Vaccine Provides Incomplete Protection in Mice and Induces Increased Eosinophilic Proinflammatory Pulmonary Response upon Challenge. *Journal of Virology*. **85** (2011), pp. 12201–12215.

13. A. Fontanet, L. Tondeur, Y. Madec, R. Grant, C. Besombes, N. Jolly, S. F. Pellerin, M.-N. Ungeheuer, I. Cailleau, L. Kuhmel, Others, Cluster of COVID-19 in northern France: A retrospective closed cohort study. *medRxiv* (2020) (available at https://www.medrxiv.org/content/10.1101/2020.04.18.20071134v1.abstract).

14. L. Grzelak, S. Temmam, C. Planchais, C. Demeret, SARS-CoV-2 serological analysis of COVID-19 hospitalized patients, pauci-symptomatic individuals and blood donors. *medRxiv* (2020) (available at https://www.medrxiv.org/content/10.1101/2020.04.21.20068858v1?rss=1).

15. info coronavirus covid 19 - carte et donnees covid 19 en france. *Gouvernement.fr*, (available at https://www.gouvernement.fr/info-coronavirus/carte-et-donnees).

Acknowledgements

Funding: We acknowledge financial support from the Investissement d'Avenir program, the Laboratoire d'Excellence Integrative Biology of Emerging Infectious Diseases program (Grant ANR-10-LABX-62-IBEID), Santé Publique France, the INCEPTION project (PIA/ANR-16-CONV-0005) and the European Union's Horizon 2020 research and innovation programme under grant agreement No 101003589. HS acknowledges support from the European Research Council (No. 804744) and University of Cambridge COVID-19 Rapid Response Grant. **Author contributions:** HS, CTK and SC conceived the study, developed the methods, performed analyses and co-wrote the paper. NL, NC, NH, AA, PB, JP, JR, C-LD, LO, PYB, AF, JL,DLB, YLS contributed to data collection and analysis. All authors contributed to paper revisions. **Competing interests:** The authors declare no competing interests. **Code and data** for the paper is available at DOI: 10.5281/zenodo.3813815.

Figure legends

Figure 1. COVID-19 hospitalizations and deaths in France (A) Cumulative number of general ward and ICU hospitalizations, ICU admissions and deaths from SARS-CoV-2 in France. The green line indicates the time when the lockdown was put in place in France. **(B)** Distribution of deaths in France. Number of **(C)** hospitalizations, **(D)** ICU and **(E)** deaths by age group and sex in France.

Figure 2. Probabilities of hospitalization, ICU admittance and death. (A) Probability of hospitalization among those infected as a function of age and sex. **(B)** Probability of ICU admission among those hospitalized as a function of age and sex. **(C)** Probability of death among those hospitalized as a function of age and sex. **(D)** Probability of death among those infected as a function of age and sex. For each panel, the black line and grey shaded region represents the overall mean across all ages. The boxplots represent the 2.5, 25, 50, 75 and 97.5 percentiles of the posterior distributions.

Figure 3. Time course of the SARS-CoV-2 epidemic to 11 May, 2020. (A) Daily admissions in ICU in metropolitan France. **(B)** Number of ICU beds occupied in metropolitan France. **(C)** Daily hospital admissions in metropolitan France. **(D)** Number of general ward beds occupied in metropolitan France **(E)** Daily new infections in metropolitan France (logarithmic scale). **(F)** Predicted proportion of the population infected by May 11th 2020 for each of the 13 regions in metropolitan France. **(G)** Predicted proportion of the population infected in metropolitan France. The black circles in panels A, B, C and D represent hospitalization data used for the calibration and the open circles hospitalization data that were not used for calibration. The dotted lines in panels E and G represent the 95% uncertainty range stemming from the uncertainty in the probability of hospitalization following infection.

Figure 4. Sensitivity analyses considering different modelling assumptions (A) Infection fatality rate (%) **(B)** Estimated reproduction numbers before (R_0) and during lockdown ($R_{lockdown}$). **(C)** Predicted daily new infections on May 11th. **(D)** Predicted proportion of the population infected by May 11th. The different scenarios correspond to: Children less inf. - Individuals <20ya are half as infectious as adults ; No Change CM - the structure of the contact matrix is not modified by the lockdown ; CM SDE - Contact matrix after lockdown with very high social distancing of the elderly ; Constant AR - Attack rates are constant across age groups ; Higher IFR- French people 25% more likely to die than Diamond Princess passengers ; Higher AR DP - 25% of the infections were undetected on the Diamond Princess cruise ship ; Delay Distrib - Single hospitalization to death delay distribution; Higher delay to hosp - 8 days on average between symptoms onset and hospitalization for patients who will require an ICU admission and 9 days on average between symptoms onset and hospitalization for the patients who will not. For estimates of IFR and reproduction numbers before and during lockdown, we report 95% credible intervals. For estimates of daily new infections and proportion of the population infected by May 11th, we report the 95% uncertainty range stemming from the uncertainty in the probability of hospitalization given infection.

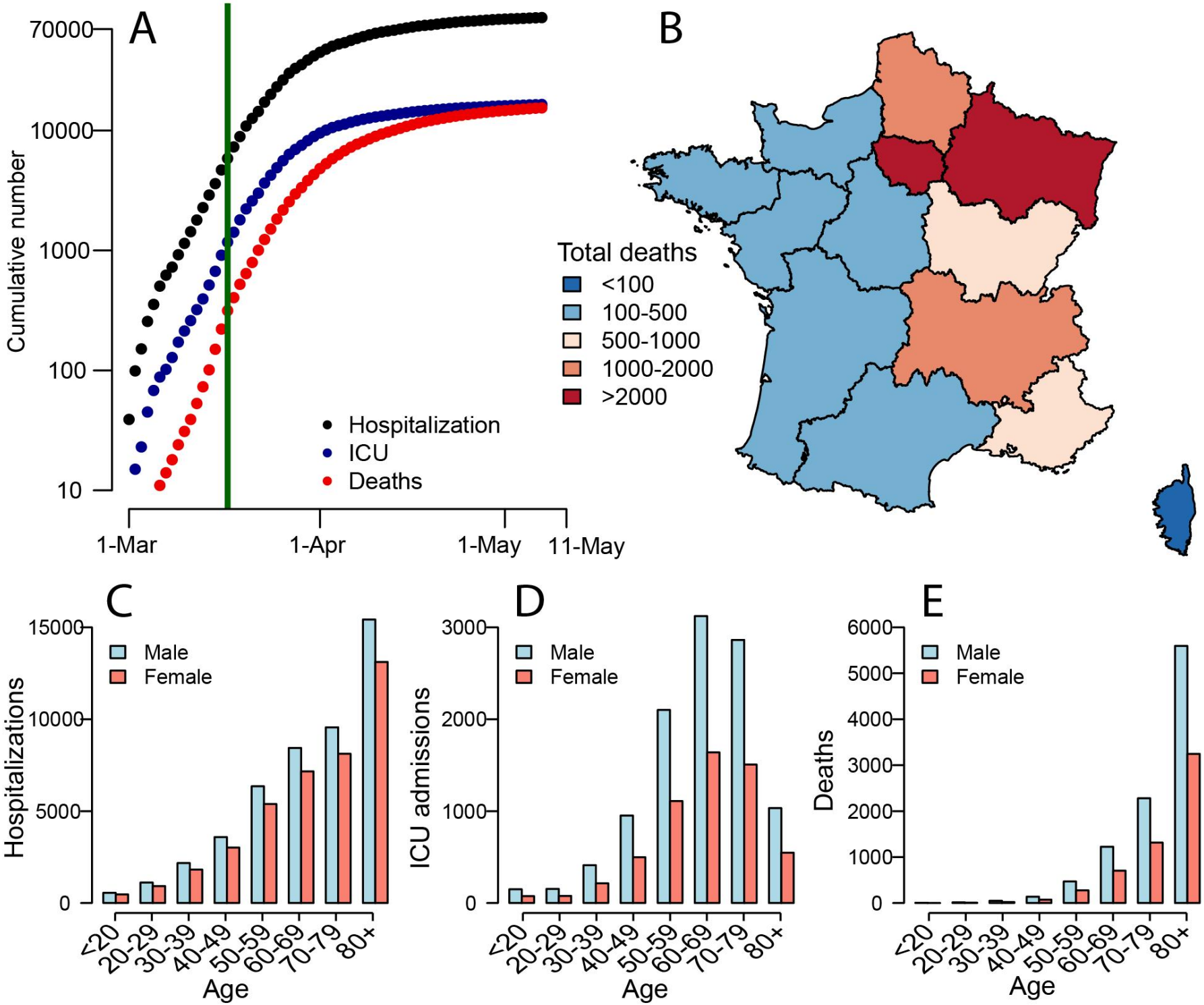
A
70000
10000
1000
100
10
Cumulative number
Hospitalization
ICU
Deaths
1-Mar
1-Apr
1-May
11-May
B
Total deaths
<100
100-500
500-1000
1000-2000
>2000
C
15000
10000
5000
0
Hospitalizations
Male
Female
<20
20-29
30-39
40-49
50-59
60-69
70-79
80+
Age
D
3000
2000
1000
0
ICU admissions
Male
Female
<20
20-29
30-39
40-49
50-59
60-69
70-79
80+
Age
E
6000
5000
4000
3000
2000
1000
0
Deaths
Male
Female
<20
20-29
30-39
40-49
50-59
60-69
70-79
80+
Age

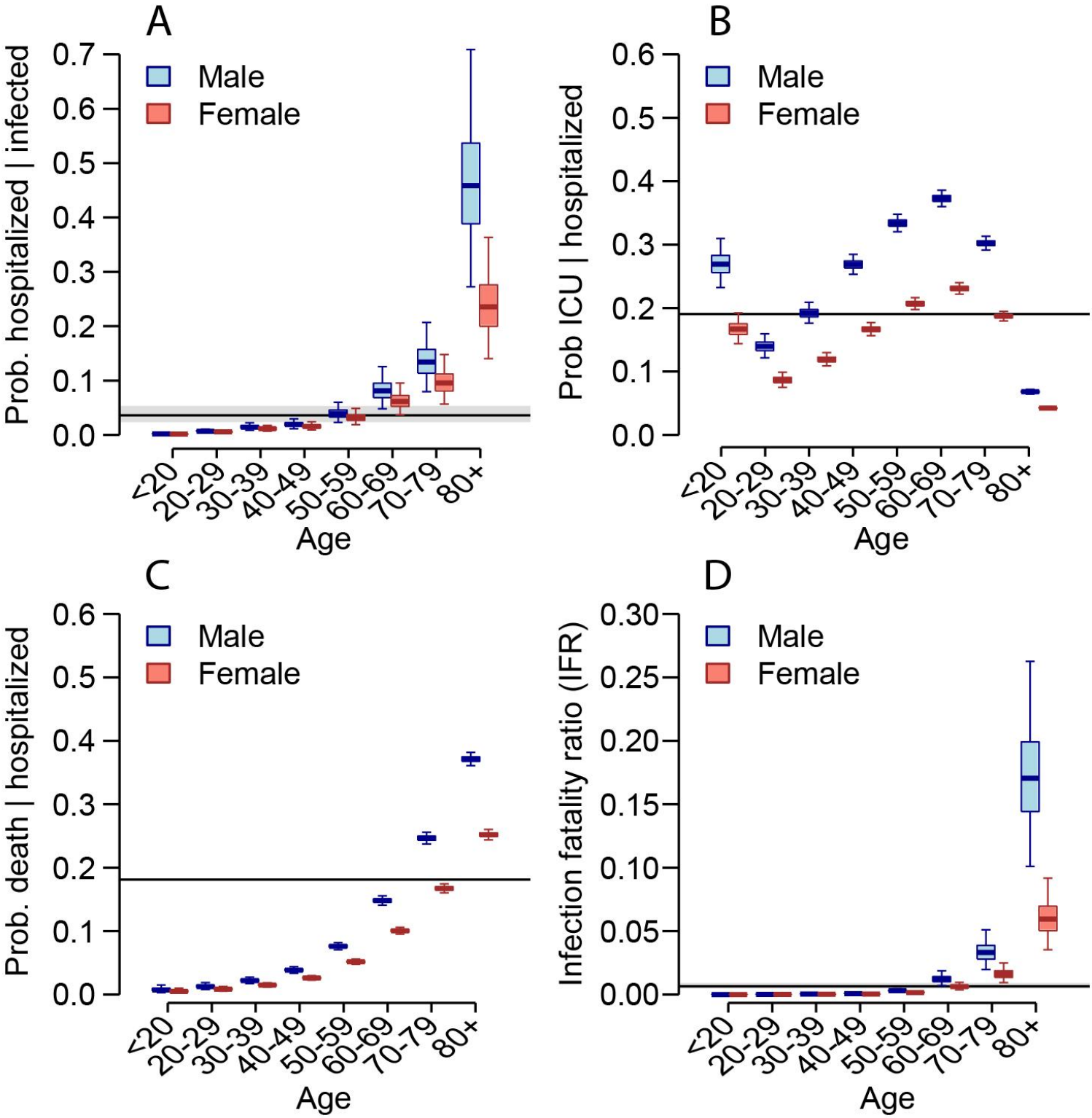
A
Prob. hospitalized | infected
0.0
0.1
0.2
0.3
0.4
0.5
0.6
0.7
Male
Female
<20
20-29
30-39
40-49
50-59
60-69
70-79
80+
Age
B
Prob ICU | hospitalized
0.0
0.1
0.2
0.3
0.4
0.5
0.6
Male
Female
<20
20-29
30-39
40-49
50-59
60-69
70-79
80+
Age
C
Prob. death | hospitalized
0.0
0.1
0.2
0.3
0.4
0.5
0.6
Male
Female
<20
20-29
30-39
40-49
50-59
60-69
70-79
80+
Age
D
Infection fatality ratio (IFR)
0.00
0.05
0.10
0.15
0.20
0.25
0.30
Male
Female
<20
20-29
30-39
40-49
50-59
60-69
70-79
80+
Age

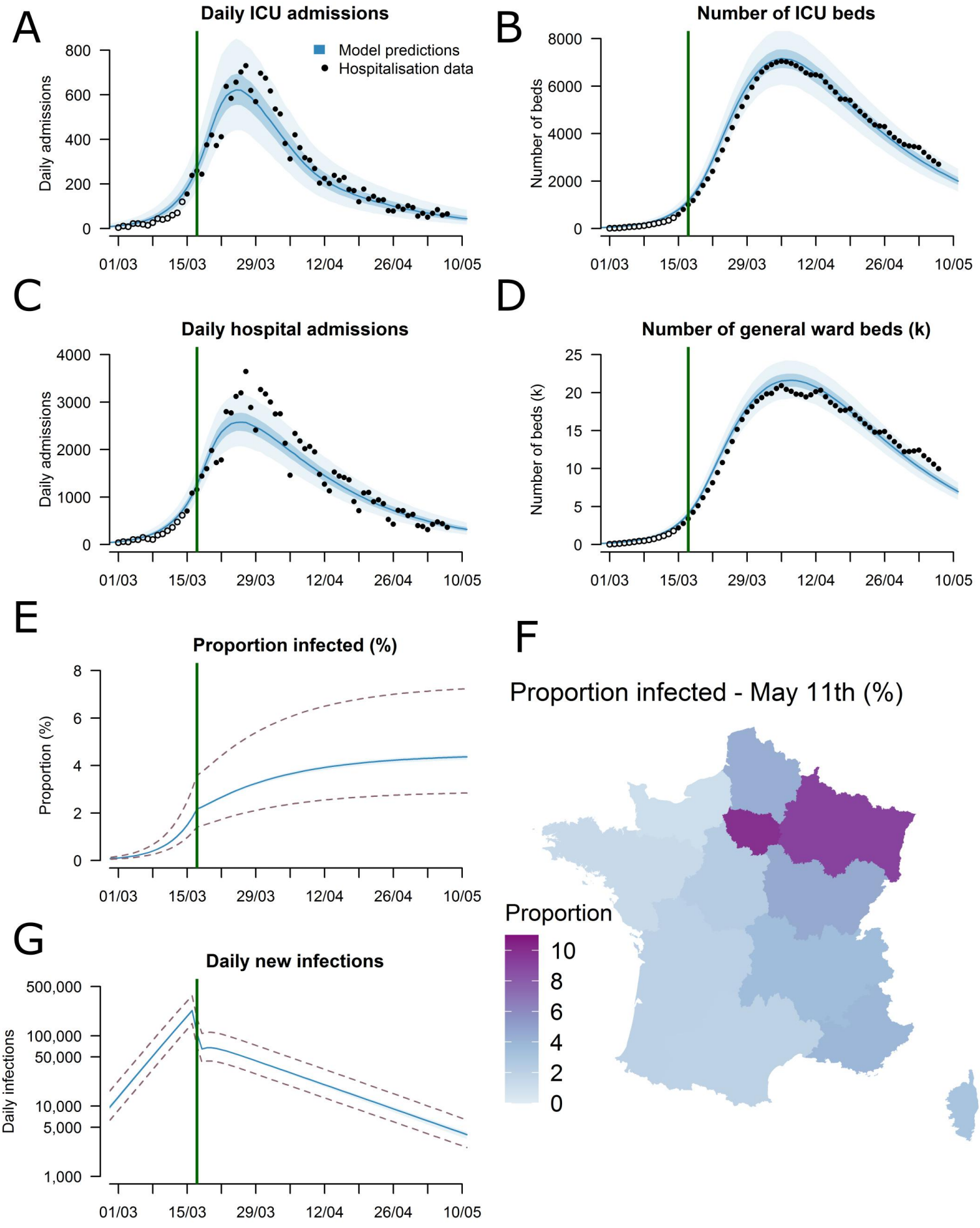
A
Daily ICU admissions
Model predictions
Hospitalisation data
Daily admissions
800
600
400
200
0
01/03
15/03
29/03
12/04
26/04
10/05
B
Number of ICU beds
Number of beds
8000
6000
4000
2000
0
C
Daily hospital admissions
4000
3000
2000
1000
D
Number of general ward beds (k)
Number of beds (k)
25
20
15
10
5
E
Proportion infected (%)
Proportion (%)
8
6
4
2
F
Proportion infected - May 11th (%)
Proportion
10
8
6
4
2
0
G
Daily new infections
Daily infections
500,000
100,000
50,000
10,000
5,000
1,000

A
IFR (%)
1.5
1.0
0.5
0.0
Baseline
Children less inf
No Change CM
CM SDE
Constant AR
Higher IFR
Higher AR DP
Delay Distrib
Higher delay to hosp

B
Reproduction numbers
R_0
$R_{lockdown}$
4
3
2
1
0
Baseline
Children less inf
No Change CM
CM SDE
Constant AR
Higher IFR
Higher AR DP
Delay Distrib
Higher delay to hosp

C
Daily infections (k)
10
8
6
4
2
0
Baseline
Children less inf
No Change CM
CM SDE
Constant AR
Higher IFR
Higher AR DP
Delay Distrib
Higher delay to hosp

D
Proportion infected (%)
10
8
6
4
2
0
Baseline
Children less inf
No Change CM
CM SDE
Constant AR
Higher IFR
Higher AR DP
Delay Distrib
Higher delay to hosp

Science
AAAS

Supplementary Materials for

Estimating the burden of SARS-CoV-2 in France

Henrik Salje, Cécile Tran Kiem, Noémie Lefrancq, Noémie Courtejoie, Paolo Bosetti, Juliette Paireau, Alessio Andronico, Nathanaël Hozé, Jehanne Richet, Claire-Lise Dubost, Yann Le Strat, Justin Lessler, Daniel Levy Bruhl, Arnaud Fontanet, Lulla Opatowski, Pierre-Yves Boelle, Simon Cauchemez

Correspondence to: simon.cauchemez@pasteur.fr

This PDF file includes:

Materials and Methods

Case data

We work with daily hospitalization and death data from the SI-VIC database, maintained by the ANS (Agence du Numérique en Santé, formerly named ASIP) and sent daily to Santé Publique France, the French national public health agency. This database provides real time data on the COVID-19 patients hospitalized in French public and private hospitals, including their age, date of hospitalization, outcome and region. All cases are either biologically confirmed or present with a computed tomographic image highly suggestive of SARS-CoV-2 infection. The SI-VIC web portal was activated for the COVID-19 epidemic on 13 March 2020, with a progressive increase in the number of hospitals transmitting data. In our analyses, we include general ward (*"Hospitalisation conventionnelle"*) and ICU patients (*réanimation, soins intensifs or unité de surveillance continue)*". We exclude patients hospitalized in psychiatric care ("*Hospitalisation psychiatrique*"), long-term care and rehabilitation care ("*Soins de suite et réadaptation*") and emergency care patients ("*Soins aux urgences*"). Individuals whose only known status was deceased or discharged (3% of patients) were attributed a hospitalization date equal to the date of discharge or death. This group generally represents individuals who died on route to the hospital or shortly thereafter or were discharged shortly after arrival.

We correct the observed time series for reporting delays. Let $H_{t,T}$denote the number of hospital admissions that were reported for time t at time $T$of the epidemic ($t \leq T$). Let $p_{t,T}$denote the probability that a hospital admission that occured at time t has been reported before time T. We estimate this probability from the cumulative distribution of hospital admissions reporting delays estimated from the SI-VIC database. We correct the observed time series of hospital admissions at time T by sampling the expected number of hospital admissions at time t $\underline{H}_{t,T}$ that have not been reported yet from:

$$\underline{H}_{t,T} \sim NB(H_{t,T}, p_{t,T})$$

where $NB$is a negative binomial distribution. We then compute the expected number of hospital admissions corrected for reporting delays as:

$$\widehat{H}_{t,T} = \underline{H}_{t,T} + H_{t,T}$$

In order to take into account the variations of the reporting delays with the day of the week (from e.g., reduced reporting over weekends), we estimate different probabilities $p_{t,T}$ according to the day of the week of t and T. We apply the same method to correct the daily time series of ICU admissions, deaths and discharges, as well as ICU releases in order to compute the corrected times series of occupied ICU and general ward beds.

Active surveillance data

The Diamond Princess is a cruise ship that suffered a SARS-CoV-2 outbreak in early February 2020. All individuals on board were tested. Out of 3711 passengers, 712 tested positive (*16*, *17*). The age distribution of the positive individuals is available for a subset of 634 individuals. We assume that the age distribution of the remaining 78 individuals who tested positive is the same. So far there have been 14 deaths, seven were individuals in their 70s, four were in their 80s, one in their 60s. No age was reported for two deaths. Four individuals remain in ICU, over two months since they disembarked from the cruise liner. As it is unlikely that individuals ultimately survive after such long durations in ICU, we consider that the total final death count will be 18. See section "*On the use of the Diamond Princess and French hospitalization data in calculating infection fatality ratios"* below for details on how these data are analyzed.

Estimating delays from hospitalization to death and from hospitalization to ICU

To estimate the delay to death for the different age groups, we use data from 11324 cases throughout France that had dates of hospitalization and dates of death recorded. We use the number of hospitalizations on a given day to account for the state of the epidemic at that time, similar to what has previously been used (*6*)(*7*). We note that a subset of individuals die within a short period of time after entering hospital. We therefore use a mixture distribution composed of an exponential distribution for those that die within a short delay and a lognormal distribution for those that die after longer delays (Figure S3). We truncate the overall distribution to 60 days.

$$\pi_i^{true} = (1-\rho)Exp(m) + \rho\, Lognormal(\mu, \sigma^2)$$

We denote by ${\pi_i}^{true}$ the true probability density function (pdf) of the delay, and ${\pi_i}^{obs}$ the observed density, which will be biased to be right skewed as some individuals will not have had their outcome. We denote by ${\Pi_i}^{true}$ and ${\Pi_i}^{obs}$ their cumulative density functions (cdf), respectively. We can approximate the expected delay distribution ${\pi_i}^{exp}$, for a given age group i, at a given time T during the epidemic, thereby adjusting for the stage of the epidemic, given the true pdf for the delay ${\Pi_i}^{true}$ using the following adjustment:

$$\pi_i^{exp}(k) = \frac{\sum_{j=1}^{T} H_{i,j-k} \times \left(\Pi_{\mathrm{i,k+1}}^{\mathrm{true}} - \Pi_{i,k}^{\mathrm{true}}\right)}{\sum_{j=1}^{T}\sum_{l=0}^{j-1} H_{i,j-l} \times \left(\Pi_{\mathrm{i,l+1}}^{\mathrm{true}} - \Pi_{i,l}^{\mathrm{true}}\right)} \quad , \qquad for\ all\ delays\ k \in [0,T]$$

where $H_{i,j}$ is the total number of hospitalized cases of age i at time j.

For the correct pdf ${\Pi_i}^{true}$, we should have:

$$\pi_i^{exp} = \pi_i^{obs}$$

We estimate parameters of the true delay from hospitalization to death distribution $\pi_i{}^{true}$ for each group in turn by minimizing the sum of squared error (SSE) of the distribution $\pi_i{}^{exp}$ to the observed data $\pi_i{}^{obs}$. Given the small number of deaths in younger age groups, we consider three age groups: <70y, 70-80, 80+. To get an overall estimate, we also repeat the calculation using all individuals across all age groups. We also consider a sensitivity analysis where we fit a single exponential distribution (Figure S14). To fit the delays from hospitalization to ICU admission we use the same approach, however, we consider the delays are constant across age groups and that they follow an exponential distribution (Figure S1).

While it would be interesting to better understand the group of patients that died quickly, unfortunately the analyzed datasets do not include information on potential factors that could lead to rapid death (e.g., data on underlying comorbidities, source of infection).

On the use of the Diamond Princess and French hospitalization data in calculating infection fatality ratios

Information for calculating the infection fatality ratio, comes both from the Diamond Princess and the age distribution of the French hospitalized population. For the underlying probability of infection in France, we assume an independent process linked to the number of contacts per day. In this way, the fact we observe few hospitalisations in younger individuals relative to older individuals and few deaths given hospitalisation in younger individuals relative to older individuals provides some information on the IFR. For example, if we assume the extreme scenario that all >80 males are hospitalised (the group with most deaths), this would still mean that the maximum IFR for those <20ya would be 0.01% (and an overall IFR of 1.3%, which could be considered an upper bound for the IFR). The Diamond Princess data helps inform the model by allowing for the fact that, given the age and sex structure of the infected passengers, the observed probability of death aboard the Princess Diamond is lower than this extreme.

Nevertheless, if the population on board the Diamond Princess is substantially healthier (e.g., with fewer comorbidities) than the average French population, this could lead to under-estimating the IFR for France. We therefore conduct a sensitivity analysis where we assume the passengers had 0.75 times the probability of death following infection, compared to French citizens (to reflect a 25% difference in the underlying frailties of the two populations). We also conduct a separate sensitivity analysis where the underlying number of infections was under-estimated due to false-negativity from PCR-based assays (but all deaths are detected). For this second sensitivity analysis, we assume that 25% of infections were missed, with the age and sex distribution of the missed infections, equal to those that were observed.

Modeling the risk of hospitalization, ICU admission and death

We consider the population of mainland France for the transmission model in eight age bands (<20y, 20-29, 30-39, 40-49, 50-59, 60-69, 70-79, 80+) and consider males and females separately. We exclude the population in retirement communities (N=730,000 individuals, mainly over the age

of 70 and 74% female), as there have been a number of outbreaks in these enclosed communities and the underlying risk of infection in these locations is unlikely to be the same as the wider population. Deaths in these communities are not captured in hospital records. Outside retirement communities, we assume that all recorded deaths occurred in hospital and that the probability of death is linked to age and sex.

For the passive French hospital surveillance system, we use a Poisson Likelihood for the number of hospitalizations, ICU admissions and deaths within each age group and sex.

$$Number\ Hospitalized\ age_{i,j} \sim Poisson\left(Population\ age_{i,j} \cdot \mu_{Hosp,i,j}\right)$$

$$Number\ ICU\ age_{i,j} \sim Poisson\left(Population\ age_{i,j} \cdot \mu_{ICU,i} \cdot \mu_{Hosp,i,j} \cdot \gamma_{ICU,j} \cdot \theta_2\right)$$

$$Number\ Death\ age_{i,j} \sim Poisson\left(Population\ age_{i,j} \cdot \mu_{Death,i} \cdot \mu_{Hosp,i,j} \cdot \gamma_{Death,j} \cdot \theta_{1,i}\right)$$

Where $\mu_{Hosp,i,j}$ is the overall probability of hospitalization for COVID19 for an individual within the population of age group *i* of sex *j*, $\mu_{ICU,i}$ is the probability of entering ICU and $\mu_{Death,i}$ is the probability of death for individuals hospitalized for COVID19 within age group *i* of sex *j*; $\gamma_{ICU,j}$ is the relative risk of entering ICU among those hospitalized for COVID19 for sex j (and kept at 1.0 for males) and $\gamma_{Death,j}$ is the relative risk of death among those hospitalized for COVID19 for sex j (and kept at 1.0 for males). θ_2 is the proportion of hospitalized individuals in the dataset that have experienced their ICU outcome and $\theta_{1,i}$ is the proportion of individuals of age group *i* that have experienced their death outcome.

As this is an ongoing epidemic, many of the hospitalizations may yet end up being fatal. To adjust for this, we estimate the proportion of current hospitalizations where the outcome is known (*18*).

$$\theta_{1,i} = \frac{\sum_{j=0}^{T} \sum_{k=0}^{\infty} c_{i,j-k}\, \pi_{i,k}}{\sum_{j=0}^{T} c_{i,j}}$$

Where $C_{i,j}$ is the number of cases at time *j* of age *i* and $\pi_{i,k}$is the proportion of all hospitalized cases in our dataset of age *i* that have a delay between hospitalization and death of *k* days. We take a similar approach to estimate the proportion of hospitalized individuals who have experienced their ICU outcome (θ_2).

The probability of death given infected ($IFR_{i,j}$) can be calculated as:

$$IFR_{i,j} = \frac{\mu_{Hosp,i,j} \cdot \mu_{Death,i} \cdot \gamma_{Death,j}}{\Lambda_i}$$

Where Λ_i is the probability of infection for an individual within age group *i* and can be expressed as:

$$P\left(Infection | Age_i \right) = \Lambda_i = \overline{\Lambda} \cdot \beta_i$$

Where $\underline{\Lambda}$ represents the mean cumulative probability of having been infected across the entire population and β_i represents the relative risk of infection for an individual of age *i* compared to a randomly selected person from the population. As SARS-CoV-2 is principally transmitted from close contact between individuals, we assume that the probability of infection is proportional to the number of contacts an individual makes. For β_i, we use the estimated number of contacts made by individuals within an age group, as measured through pre- and post-lockdown contact matrices, as a proxy for the relative attack rate by age. For the pre-lockdown period, we use the mean number of contacts that an individual of age group *i* has on a daily basis as measured in France (*19*). For the post-lockdown period, we adjust the number of contacts to reflect increased time spent at home (see 'Impact of the lockdown on transmission' section below). In each case, we reweight the number of contacts by the proportion of the population that is within that age group. We justify the use of the relative number of contacts across age groups as a proxy for relative attack rate by age by noting the linear relationship between the two in simple age-structured transmission simulations with contact matrices (Figure S16). We further note that approximately 50% of infections up to the end of April occurred prior to the lockdown and therefore use a simple average between the pre- and post-lockdown contact numbers to estimate the mean relative number of contacts by age group across the epidemic.

In order to disentangle the underlying probability of infection from the probability of hospitalization and death, we use the results of an active surveillance campaign in a different population (cruise ship) where all individuals were tested, and therefore the probability of detection is not linked to the presence of severe disease that requires hospitalization.

For the active surveillance portion of the model, we use a Poisson likelihood to capture the number of deaths (Baseline scenario: N=18; see Active surveillance data section) among those infected on the Diamond Princess cruise ship. We do not consider the underlying transmission process aboard the boat so only look at the subset of the onboard population that tested positive (N=712). For 634 individuals who tested, we know their age and sex (*20*). We assume the remaining 78 positive individuals have the same age and sex distribution.

$$No.\ Death_{active} \sim$$
$$Poisson\left(\sum_j^2 \sum_i^{NGroups} No.\ infected_{active,i,j} \cdot IFR_{i,j} \right)$$

Where No. $Death_{active}$ represents the total number of deaths among infected individuals, *NGroups* is the number of age groups and *No. infected*$_{active,i,j}$ is the number of infected individuals from the Princess Diamond of age group *i* and sex *j*.

We use RStan (*21*) to fit the $\mu_{Hosp,i,j}$, $\mu_{ICU,i}$, $\mu_{Death,i}$,$\gamma_{Death,j}$,$\gamma_{ICU,j}$ and Λ parameters using logit transformed parameters for $\Lambda, \mu_{Hosp,i,j}$, $\mu_{ICU,i}$,$\mu_{Death,i}$with cauchy(0,1) priors and log-transformed

parameters for $\gamma_{Death,j}, \gamma_{ICU,j}$ with normal(0,0.5) priors. We run four chains of 10,000 iterations each and remove 50% for burn-in. We use 2.5% and 97.5% percentiles from the resulting posterior distributions for 95% credible intervals for the parameters. To calculate the overall probability of hospitalization following infection for the whole population we compute an average across the individual $\mu_{Hosp,i,j}$ estimates, weighted by the estimated number of people infected in each age-sex group. Similarly, to calculate the overall probability of death following hospitalisation, we compute an average across the individual $\mu_{Death,i}$ estimates, weighted by the estimated number of people hospitalised in each age-sex group.

Transmission model fit to hospital data

We use a deterministic compartmental model stratified by age to describe the transmission of SARS-CoV-2 in the French population. Upon infection, susceptible individuals will enter a latent compartment (first exposed compartment E_1), in which they will stay for an average of 4.0 days. During this period, they are not infectious. They will then move to a second exposed compartment E_2in which they will on average stay 1.0 day. Upon entry in the E_2 compartment, infected individuals become infectious. They then move to the compartment *I* where they stay for an average duration of 3 days, where all individuals are infectious and a subset develop symptoms. This parametrization gives a mean incubation period of 5 days and allows for one day of pre-symptomatic transmissions, in line with several estimates from Chinese data (*22*, *23*). It is also in line with generation interval estimates obtained from analyses of infector-infectee pairs from mainland China (*22*).

A subset of infected individuals develop severe disease that results in hospital admission. The probability of entering hospital depends on age ($\mu_{Hosp,i}$for age i). Some of the hospitalized patients will additionally require an ICU admission. The probability to require an ICU admission given hospitalization also depends on age ($\mu_{ICU,i}$ for age i). Finally, we assume that patients who will later be admitted in ICU enter hospital on average 6 days after disease onset, consistent with previous estimates (*24*). Patients who are hospitalized but will not require admission to ICU enter the hospital on average 7 days after symptom onset.

We assume that by the end of their infectious period (for patients who are not hospitalized) or by the end of their hospital stay (for patients who are hospitalized), individuals move to an R/D (Recovered or Deceased) compartment in which they are no longer susceptible to SARS-CoV-2 infection. The model is initiated with I_0 cases in the E_1compartment on the 22nd January 2020 (t_0).

Contacts patterns in the French population prior to the lockdown

Age-specific daily contacts for the French population are obtained from the study COMES-F performed in 2012 (*19*). From this survey, we reconstruct the contact matrix describing mixing between age classes during a non-holiday period. To compute the matrix, we divide the population equally from 0 to 80 ya into 8 classes of ten years each. For the elderly, we consider one unique class that contains over-80 ya people. Daily contacts are computed by taking into account the

variability associated with the weekend/weekdays seasonality. Data on contacts are retrieved and computed using the SocialmixR package (*25*).

Computing the transmission rate prior to the lockdown

From the definition of the contact matrix, the parametrization of our transmission model and a given reproduction number R_0, we can obtain the following expression for the transmission rate β(*26*, *27*):

$$\beta = \frac{R_0}{D \cdot max\ Eigenval\ [C]}$$

where $max\ Eigenval\ [C]$is the maximum eigenvalue of the contact matrix C and $D$is the mean infectious period.

Trajectories of patients in hospital settings

We assume that the time spent in hospital prior to admission in ICU follows an exponential distribution of mean 1.5 days (Figure S1). We assume that the time spent in ICU is constant across age-groups and that it follows a Gamma distribution of shape 2 and of rate g_{ICU}^{out}. This is modelled as two separate compartments for trajectories in ICU, from which individuals in ICU go out at rate g_{ICU}^{out}. The mean time spent in ICU is thus equal to $2/g_{ICU}^{out}$. Similarly, we assume that the time spent in general wards by hospitalized patients follows a Gamma distribution of shape 2 and of rate g_{hosp}^{out}.

We note that the proportion of patients entering ICU has changed over the epidemic (Fig S17). To account for this, we assume a change in the probability $\mu_{ICU}(t)$ of being admitted in ICU given hospitalization at time t between March 20th (t_{begin}) and April 7th (t_{end}) following a linear trend from $\mu_{ICU}^{baseline}$ to $\alpha \cdot \mu_{ICU}^{baseline}$ where $\alpha$is a parameter to be estimated. We assume that this change was similar across age-groups and across regions. For a given age-group i, the baseline probability $\mu_{ICU,i}^{baseline}$ is computed so that the average probability of entering ICU between March 1st (t_{min}) and May 7th (t_{max}) $\mu_{ICU,i}$ satisfies:

$$\mu_{ICU,i} = \frac{\sum_{t=t_{min}}^{t_{max}} \mu_{ICU,i}(t) \cdot n_{hosp}(t)}{\sum_{t=t_{min}}^{t_{max}} n_{hosp}(t)}$$

where $n_{hosp}(t)$is the number of hospitalizations on day t. Accounting for this trend is important to explain the slowing down of ICU admissions from mid April.

Impact of the lockdown on transmission

In response to the growing epidemic, from March 17th, the French population was asked to remain confined to their homes and to avoid non-essential movement outside the household (*28*). We adjusted our contact matrix to reflect the impact of the lockdown on the distribution of daily contacts between individuals after this date. We denote C, the contact matrix prior to the lockdown (*19*) and transmission rates prior to the lockdown are modelled asβC .

In order to model the impact of the lockdown on transmission, one potential approach is to predict how the standard contact matrix C is modified during the lockdown due to reductions in contacts in different settings. If we denote CL the predicted contact matrix during the lockdown period, the transmission rates for the lockdown period would then simply be βCL. However, a limitation of this approach is that given the unprecedented nature of the lockdown, it is hard to predict precisely what the new contact matrix CL may look like. Any slight error in the assumed reduction of the average number of contacts would have a strong impact on estimates of the reproduction number for the lockdown period.

To avoid such risk, we instead estimate a transmission parameter separately for the time period before (β) and during the lockdown ($\beta_{Lockdown}$). Comparison of these two parameters will determine the reduction in the reproduction number due to the lockdown. Since the reduction in average number of contacts will be captured by transmission parameters (β, $\beta_{Lockdown}$), we work with normalized contact matrices, i.e. contact matrices whose maximum eigenvalues are equal to 1. This allows us to define βas R_0/D and $\beta_{Lockdown}$ as $R_{lockdown}/D$ and to compute transmission rates before and after lockdown as βC and $\beta_{lockdown}CL$. We modify the contact matrix for the lockdown to capture the impact of the lockdown on the structure of the matrix. This normalization ensures that estimates of *R* during the lockdown are little impacted by the matrix we choose (see Figure 4).

The normalized contact matrices we consider for the lockdown matrices are:

- CL_1(baseline): the original (pre-lockdown) contact matrix by removing all contacts in school settings and further assume a reduction of 80% in the contacts associated with the workplace and 90% in the ones outside work and home. This represents our baseline assumptions for the lockdown period.
- CL_2(Children Less Inf - children less infectious): same as CL_1but where those aged <20 y.o. are 50% less infectious.
- CL_3(CM No Change - contact matrix no change): the original (pre-lockdown) contact matrix (i.e. no change in the matrix).
- CL_4(CM SDE - contact matrix social distancing elderly): same as CL_1but with a further 20% reduction in all contacts of individuals aged over 70y.
- CL_5(Constant AR - constant attack rates): all the coefficients of the contact matrix are equal to 1 (homogeneous mixing of the population).

We use Matrix CL1 for our baseline scenario(*29*). We find similar Deviance Information Criteria for the different matrices (Table S11) (29).

We estimate that the lockdown had an important impact on SARS-CoV-2 transmission in France. This is consistent with a large drop in visits to retail, recreation and work spaces after the lockdown was put in place, as measured through mobile phone tracing (*30*).

Statistical framework for the transmission model

We fit the transmission model using a Bayesian framework and jointly infer parameters. To do this we let ${Adm_{ICU}}^{pred}(t)$, ${Adm_{Hosp}}^{pred}(t)$, $ICU^{pred}(t)$and $Hosp^{pred}(t)$denote respectively the number of admissions in ICU, the number of admissions in hospital, the number of ICU beds and the number of general wards beds on day t predicted by our model. We then let ${Adm_{ICU}}^{cor}(t)$, ${Adm_{Hosp}}^{cor}(t)$, $ICU^{cor}(t)$ and $Hosp^{cor}(t)$respectively denote the corrected number of ICU admissions, the corrected number of hospital admissions, the corrected number of ICU beds and the corrected number of general ward beds occupied on day t. The likelihood function until day $T$is:

$$L_T = \prod_{t=t_1}^{T} g({Adm_{ICU}}^{cor}(t) \mid {Adm_{ICU}}^{pred}(t)) \cdot g(ICU^{cor}(t) \mid ICU^{pred}(t)) \cdot \prod_{t=t_1}^{T} g({Adm_{Hosp}}^{cor}(t) \mid {Adm_{Hosp}}^{pred}(t)) \cdot g(Hosp^{cor}(t) \mid Hosp^{pred}(t))$$

where $g(\cdot \mid X)$ is a negative binomial distribution of mean X and overdispersion parameter X^{δ}, δbeing a parameter to be estimated. We calibrate the model on corrected SI-VIC data from the 15th of March onwards (denoted t_1).

The parameter space is explored by Markov Chain Monte Carlo sampling. We implement a Metropolis-Hastings (MH) algorithm with lognormal proposals for all the parameters and uniform priors. Chains are run for 10,000 iterations with 2,000 iterations of burn-in.

In early attempts to estimate model parameters, the initial number of cases at the start of the simulation I_0 was highly correlated to the reproduction number. This is because slight variations in I_0 or the reproduction number can lead to major changes in the trajectory of cumulative number of cases. We therefore re-parameterized the model to reduce this correlation by using a proxy for the number of incident cases at the time of the lockdown $I_{lockdown}$.

$$log\ I_0 = log\ I_{lockdown} - r(t_{lockdown} - t_0)$$

Where $I_0$is the initial number of cases and *r* is the epidemic growth rate before the lockdown. We use the approach by Wallinga et al. (*31*) to relate the basic reproduction number to the epidemic growth rate r.

Incorporation of uncertainty from the probability of entering ICU following hospitalization

We incorporate uncertainty from the probability of being hospitalized following infection and in the probability of entering ICU given hospitalization in our estimates of the number of new infections and the immunity in the population over time. To do this, we separately rerun the transmission model using the 2.5% and 97.5% quantiles from the posterior of $\mu_{Hosp,i}$. The results of these estimates are included in Figures 3E, 3G, 4C,4D and S4(A-M)5-6. Uncertainty in these parameters had little effect on our estimates of the number of required ICU and general ward beds and ICU or hospital admissions.

Simulation study to assess model performance in estimating IFR and hospitalization risk

To assess the performance of the approach to estimate probabilities of infection, hospitalization, ICU entry, and death, we developed a simulation framework where the true parameters ($\mu_{Hosp,i}$, $\mu_{ICU,i}$,Λ, $\mu_{Death,i}$) were known.

For a period of 70 days we simulate an epidemic, seeded by a single infection, where the number of cases grows exponentially each day with an initial exponential growth rate of 0.2 for 40 days and a subsequent exponential growth rate of -0.1, to reflect an approximation of what has been observed in France. We assume a population with the same age structure as France and assume no difference in risk of infection by age or sex. For each of the infections in the simulation we assign:

- The age group, *i*, drawn according to the age distribution of France
- Whether or not the individual was hospitalized, using a random draw from a Bernoulli distribution with parameter $\mu_{Hosp,i}$
- If the individual was hospitalized, whether or not the individual entered ICU, using a random draw from a Bernoulli distribution with parameter $\mu_{ICU,i}$
- If the individual was hospitalized, whether or not the individual died, using a random draw from a Bernoulli distribution with parameter $\mu_{Death,i}$
- If the individual was hospitalized, the day of hospitalization using an exponential distribution with a mean of 11 days.
- If the individual entered ICU, the delay from hospitalization to ICU using a random draw from an exponential distribution with a mean of 1.5 days.
- If the individual died, the delay from hospitalization to death using a random draw from an exponential distribution with a mean of 15 days.

We then compute the total counts of hospitalizations, ICU and deaths by age over the first 70 days of the simulation (Figures S7).

To simulate active surveillance, we select a random subset of 1000 individuals that were infected and record the outcome (death or not) and age for all of them (irrespective of delays to death).

We use the simulated data to estimate the proportion of cases with outcome observed (θ) and the model parameters using our probabilistic framework.

Ethical considerations

The study was based on a secondary use of a database/pseudonymised data collected from health professionals. According to French law such studies are not required to receive ethics committee approval. In addition, the study was carried out as a contribution to the legal missions of health surveillance and alert of Santé Publique France, and therefore benefited from the legal prerogatives vested in Santé Publique France to carry out these missions. Santé Publique France can access all information, which is necessary for the accomplishment of its missions and has authorization from the French data protection authority to process personal health data in order to prevent, manage or assess the consequences of an epidemic.

Figure S1: Fit of delay from hospitalization to ICU admission.

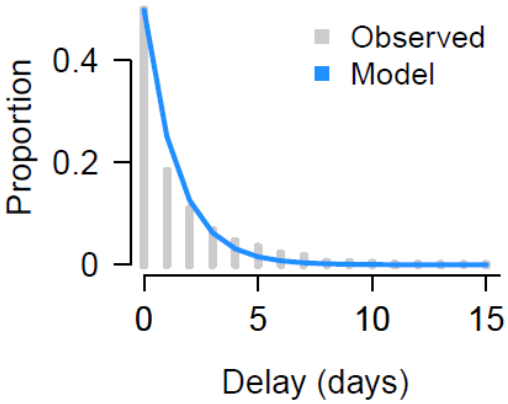

Figure S1: Model and observed fit of exponential model use times from hospitalization to ICU entry across all ages, taking account for the exponentially growing nature of the epidemic.

Figure S2: Relative differences by sex

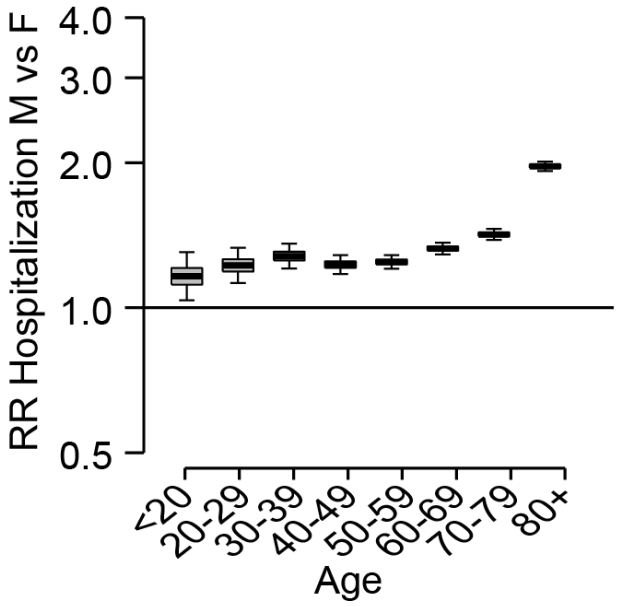

Figure S2. Relative risk of hospitalization comparing males versus females by age.

Figure S3: Fit of delays from hospitalization to death

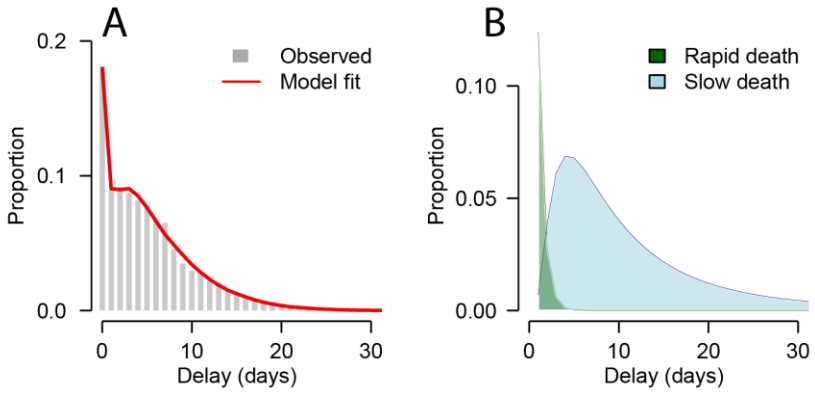

Figure S3. (A) Observed and fitted distribution of delays between hospital admission and death. **(B)** Model estimates of distribution of rapid decline and slow decline. Models fitted to take into account that in a growing epidemic, observed deaths will be biased towards ones that die quickly.

Figure S4: Fit of delays from hospitalization to death by age

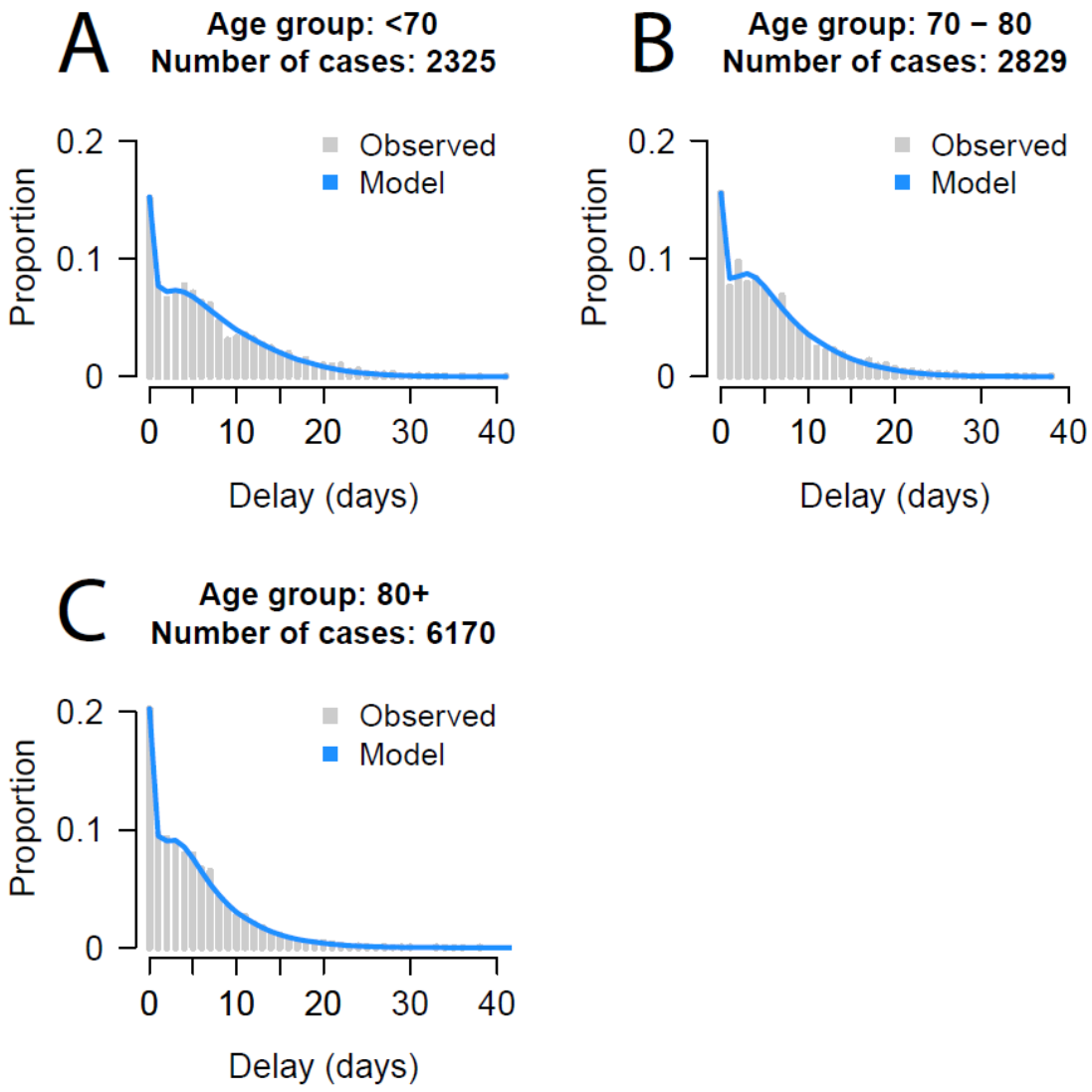

Figure S4. Fit of mixture models to time from hospitalization to death for different age groups. The models are mixture models that have both an exponential decay for those that die quickly and a log-normal component for those that die after longer delays.

Figure S5: Trajectories predicted by the regional model

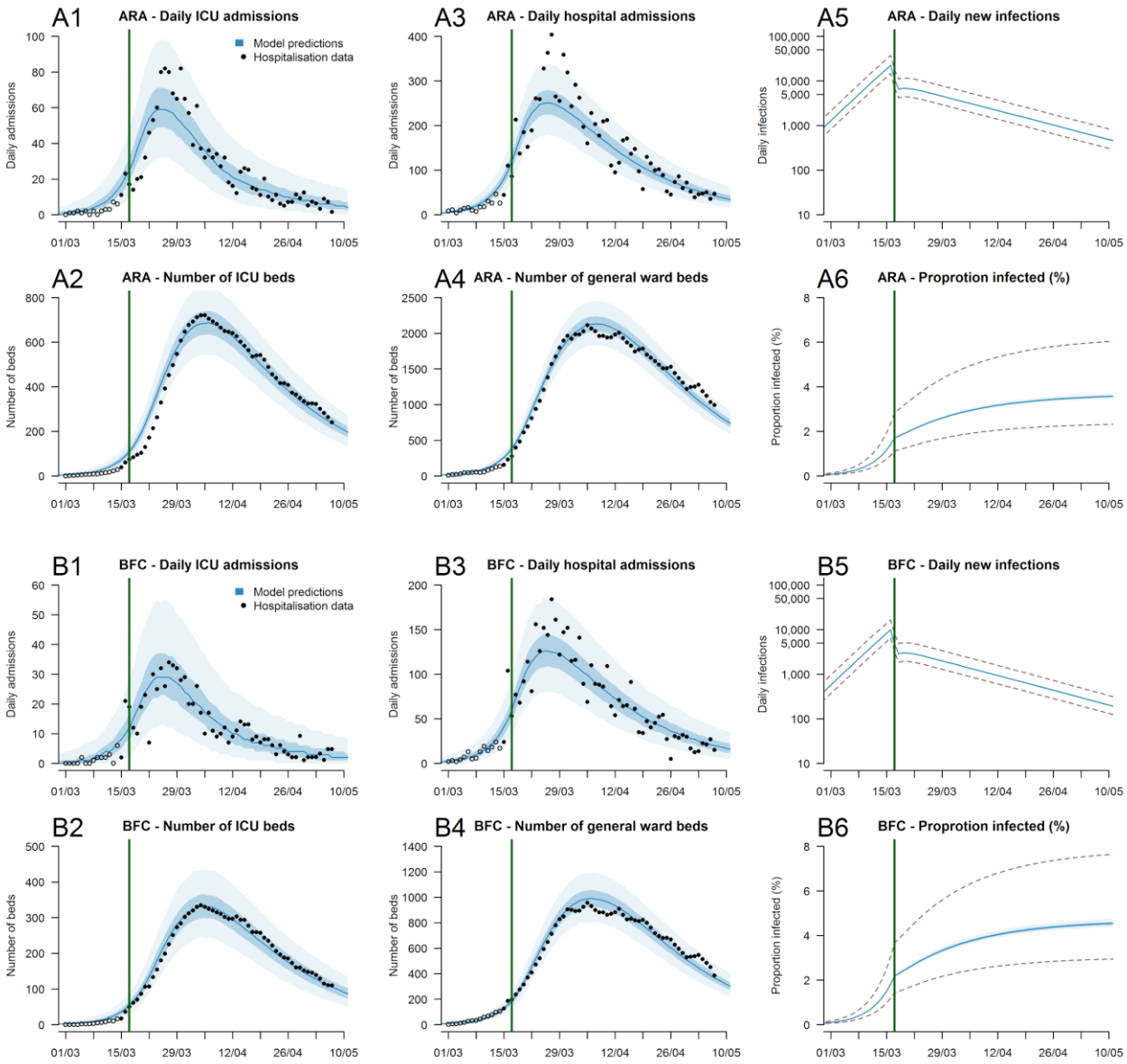

Figure S5: Predictions per French region (A) Auvergne-Rhône-Alpes ; (B) Bourgogne-Franche-Comté : (C) Bretagne : (D) Centre-Val de Loire ; (E) Corse ; (F) Grand-Est ; (G) Hauts-de-France ; (H) Île-de-France ; (I) Nouvelle-Aquitaine ; (J) Normandie ; (K) Occitanie ; (L) Provence-Alpes Côte d'Azur; (M) Pays-de la Loire. (1) Daily ICU admissions. (2) Number of ICU beds (3) Daily hospital admissions. (4) Number of general ward beds occupied (5) Daily number of infections (logarithmic scale). (6) Proportion infected. The green line indicates the time intervention measures were put in place that limited movement in the country. The dotted lines in panels 5 and 6 represent the 95% uncertainty range stemming from the uncertainty in the probability of hospitalization following infection. Note that the definition of hospitalizations differs from the one used by Santé Publique France. See the Case data section in the methods description for further details.

Figure S6: Diamond Princess fit

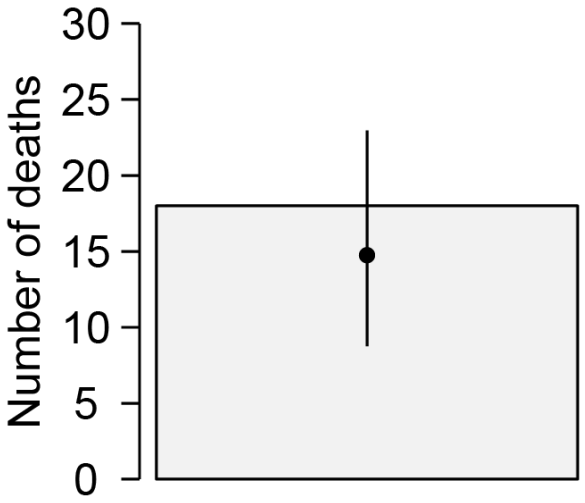

Figure S6: The assumed (grey) and fitted (black line) total number of deaths from passengers on board the Diamond Princess who were infected with SARS-CoV-2. The observed total includes four individuals that are still in ICU.

Figure S7: Simulation results

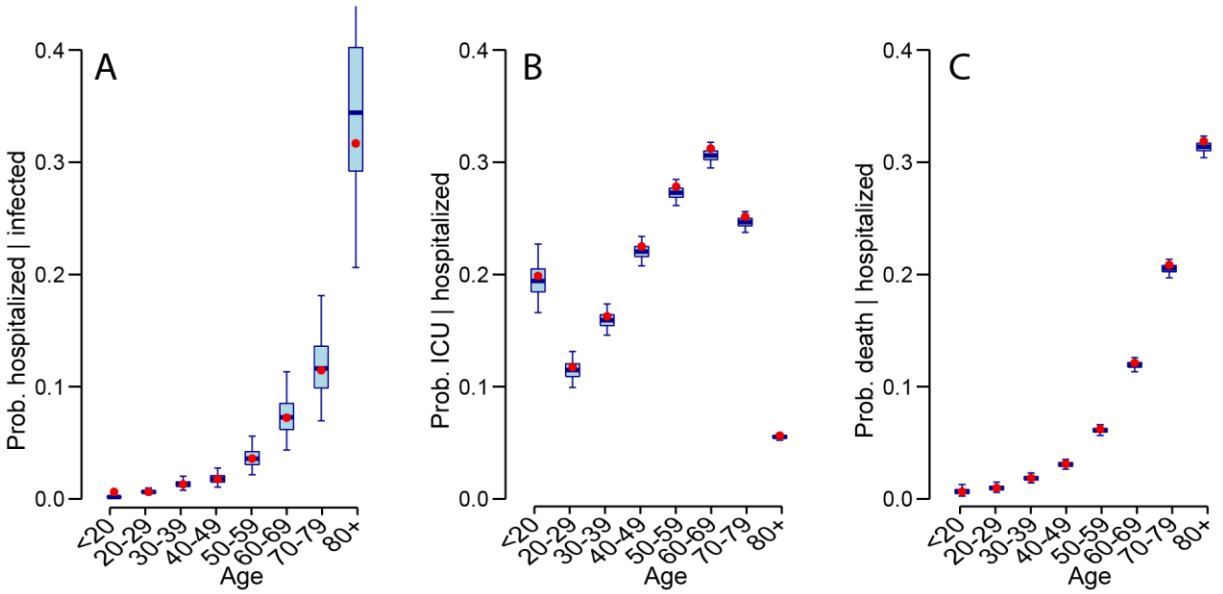

Figure S7: Simulation results where epidemics are simulated with known probabilities of infection, hospitalization, ICU and death. We then use our model framework to re-estimate the parameters. **(A)** Estimated (blue) and true (red) probability of hospitalization by age. **(B)** Estimated (blue) and true (red) probability of ICU admission by age. **(C)** Estimated (blue) and true (red) probability of death by age among those hospitalized.

Figure S8: Sensitivity analysis with additional mortality on Diamond Princess (healthier population)

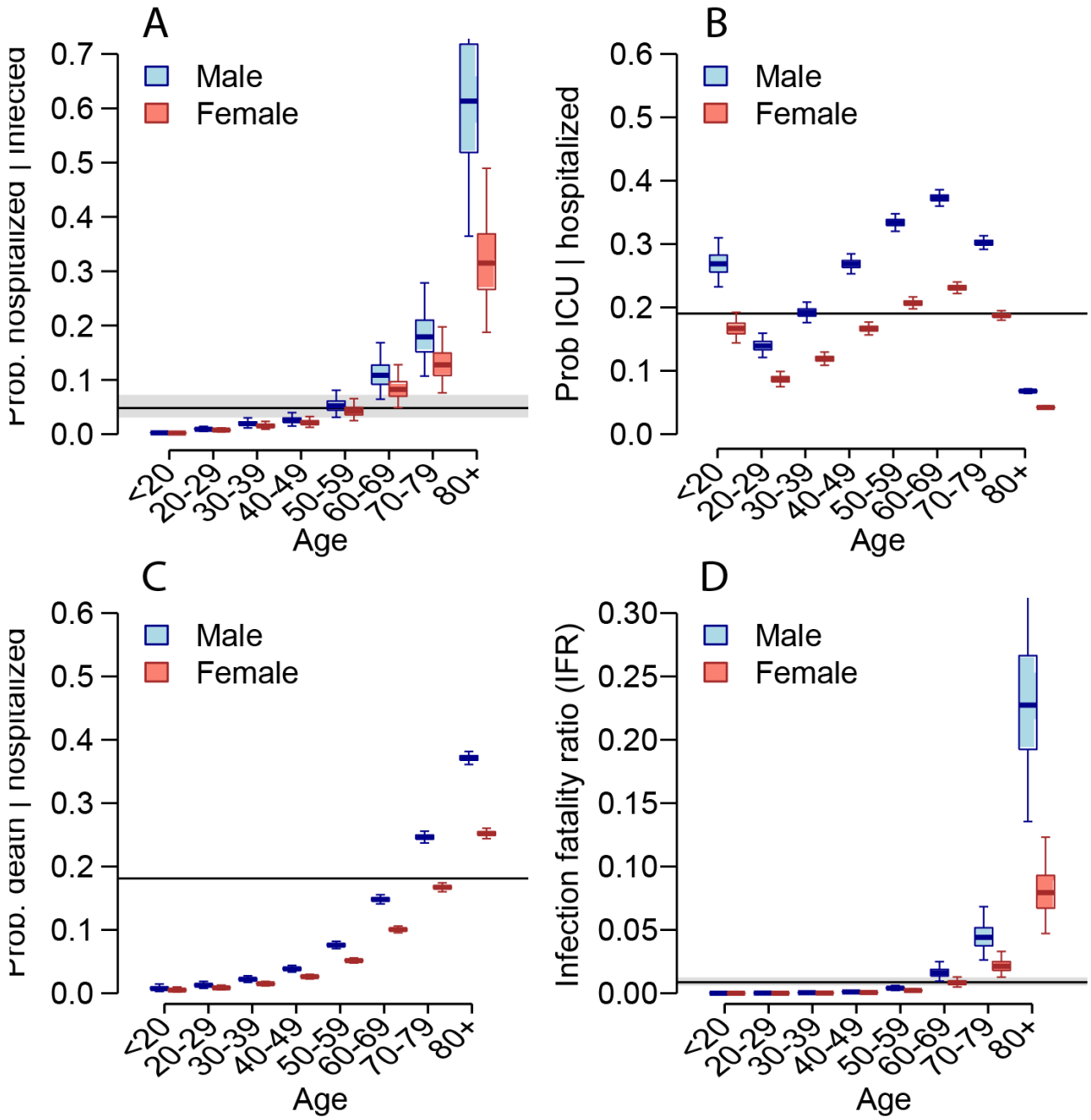

Figure S8: (A) Probability of hospitalization among those infected as a function of age and sex. **(B)** Probability of ICU admission among those hospitalized as a function of age and sex. **(C)** Probability of death among those hospitalized as a function of age and sex. **(D)** Probability of death among those infected as a function of age and sex. For each panel, the black line and grey shaded region represents the overall mean across all ages.

Figure S9: Sensitivity analysis with no change in contact matrix post lockdown

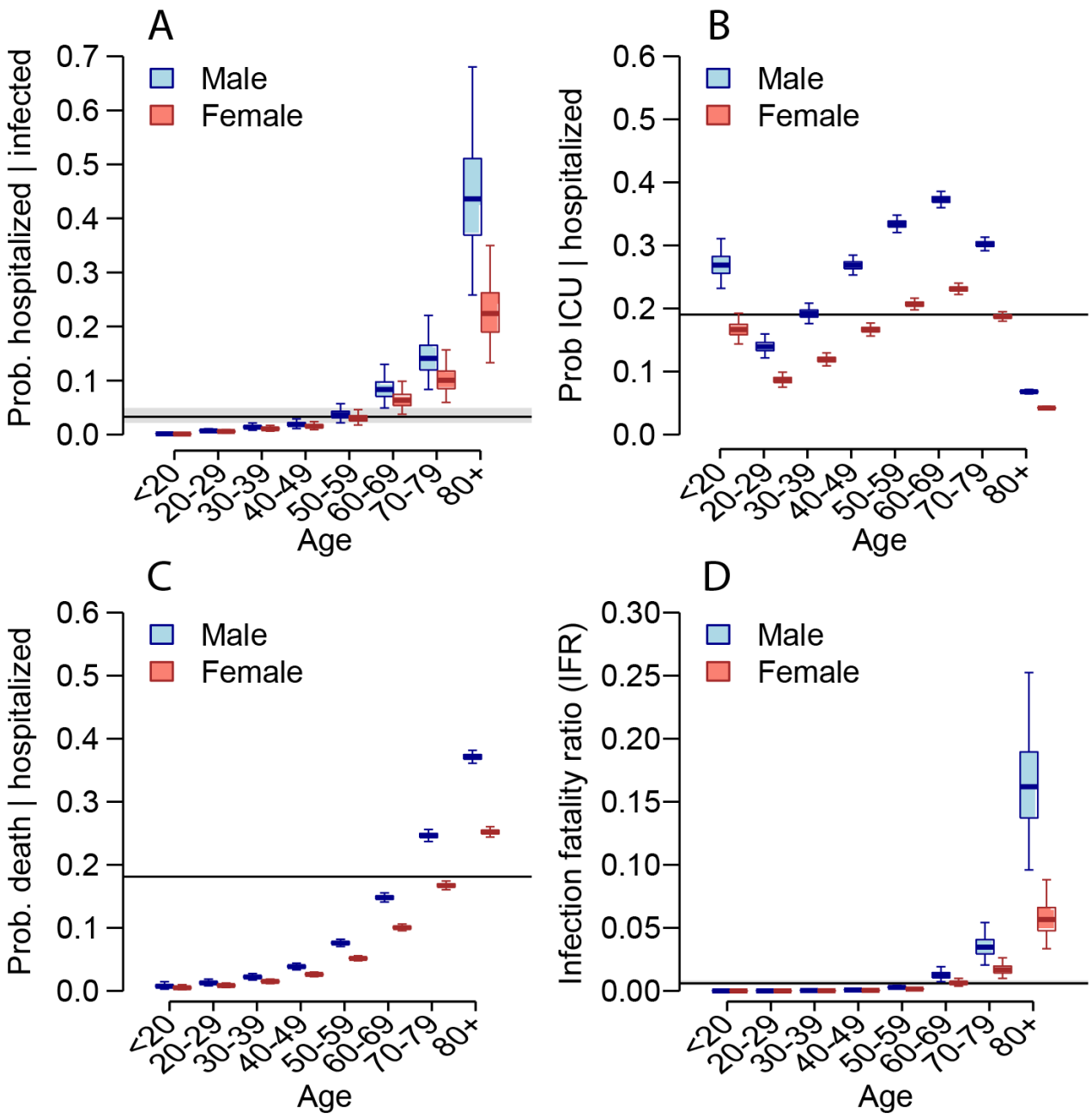

Figure S9: (A) Probability of hospitalization among those infected as a function of age and sex. **(B)** Probability of ICU admission among those hospitalized as a function of age and sex. **(C)** Probability of death among those hospitalized as a function of age and sex. **(D)** Probability of death among those infected as a function of age and sex. For each panel, the black line and grey shaded region represents the overall mean across all ages.

Figure S10: Sensitivity analysis with additional social distancing among elderly after lockdown

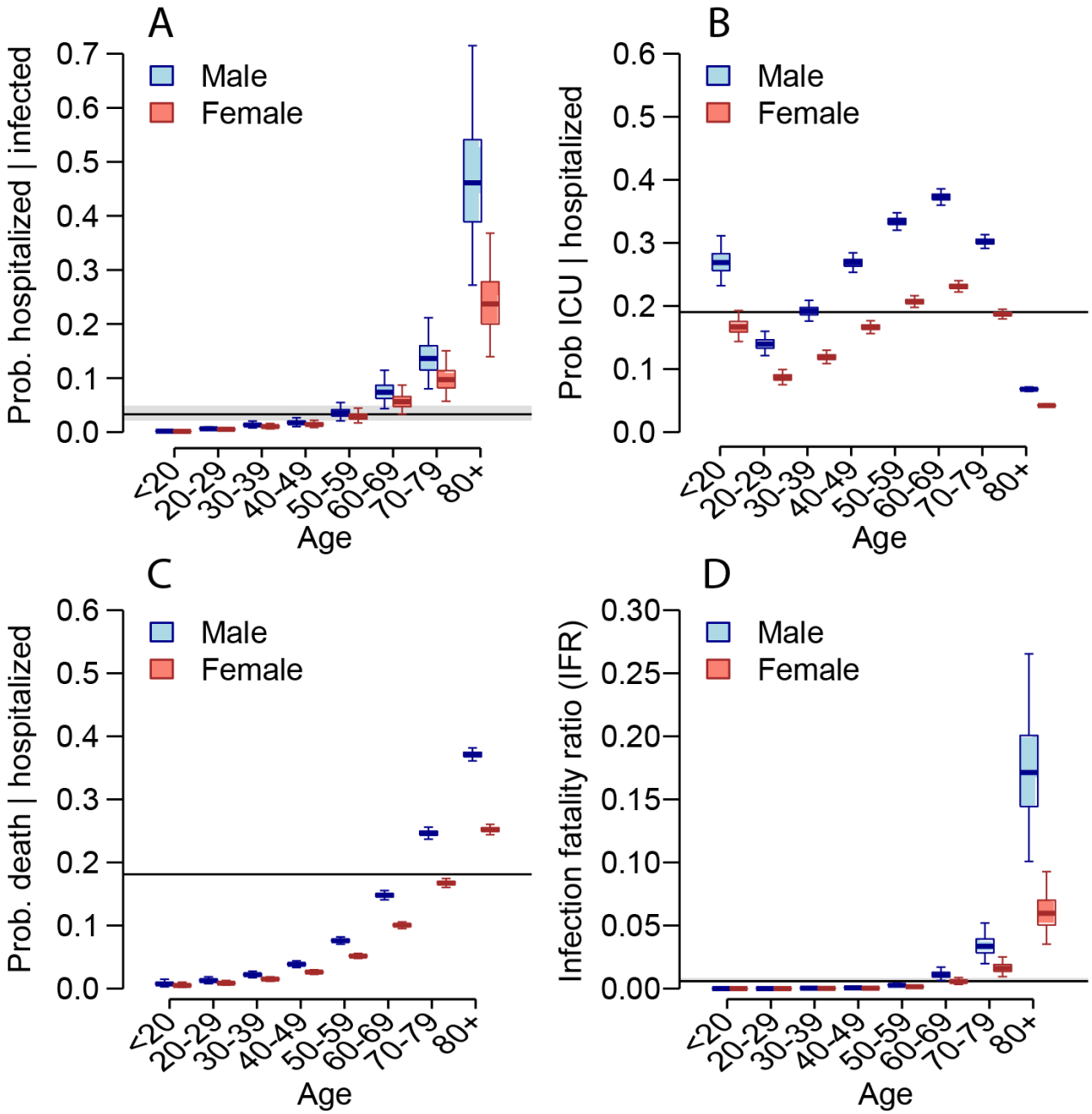

Figure S10: (A) Probability of hospitalization among those infected as a function of age and sex. **(B)** Probability of ICU admission among those hospitalized as a function of age and sex. **(C)** Probability of death among those hospitalized as a function of age and sex. **(D)** Probability of death among those infected as a function of age and sex. For each panel, the black line and grey shaded region represents the overall mean across all ages.

Figure S11: Sensitivity analysis with children less infectious than adults

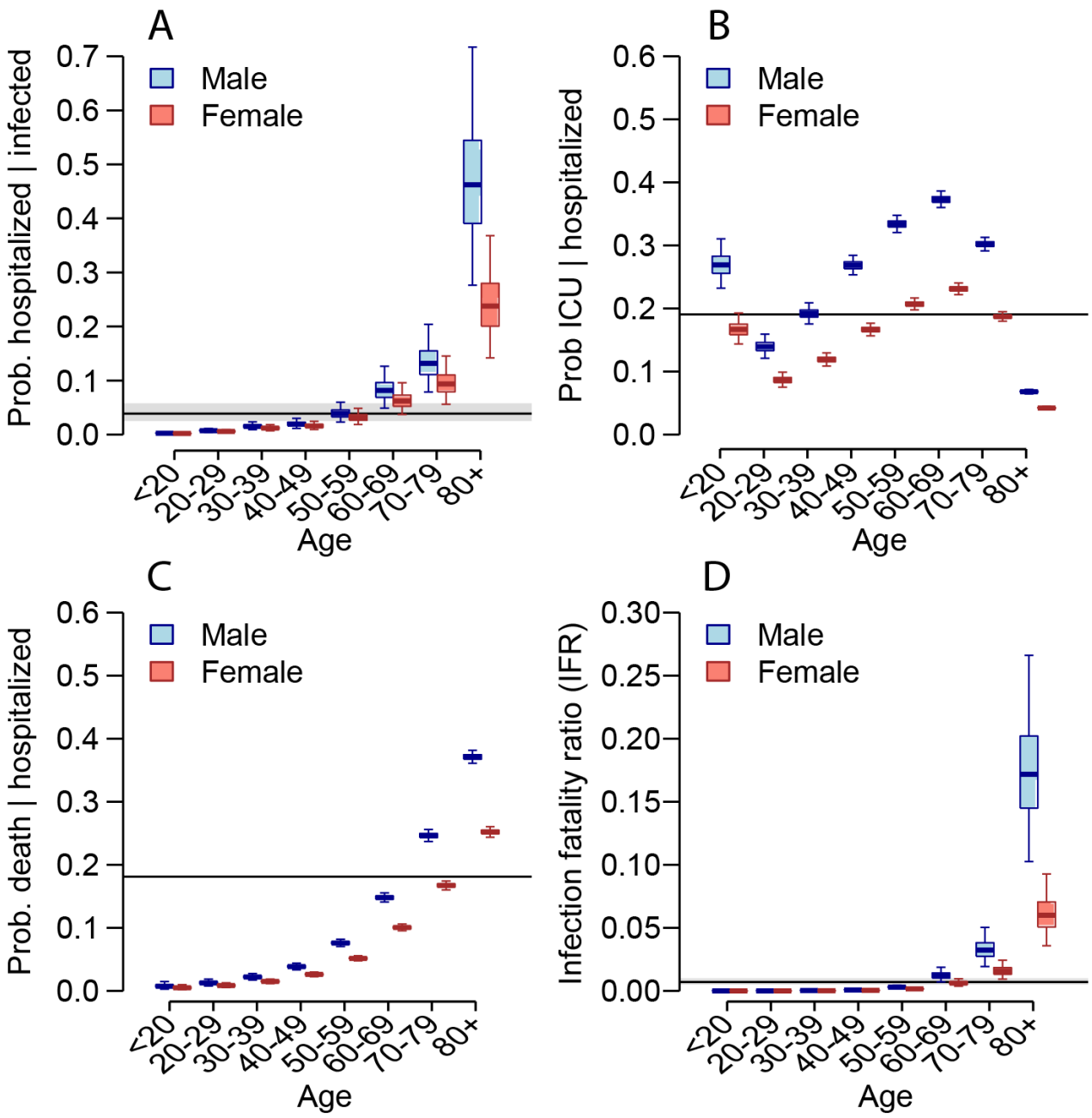

Figure S11: (A) Probability of hospitalization among those infected as a function of age and sex. **(B)** Probability of ICU admission among those hospitalized as a function of age and sex. **(C)** Probability of death among those hospitalized as a function of age and sex. **(D)** Probability of death among those infected as a function of age and sex. For each panel, the black line and grey shaded region represents the overall mean across all ages.

Figure S12: Sensitivity analysis with equal attack rates across age groups

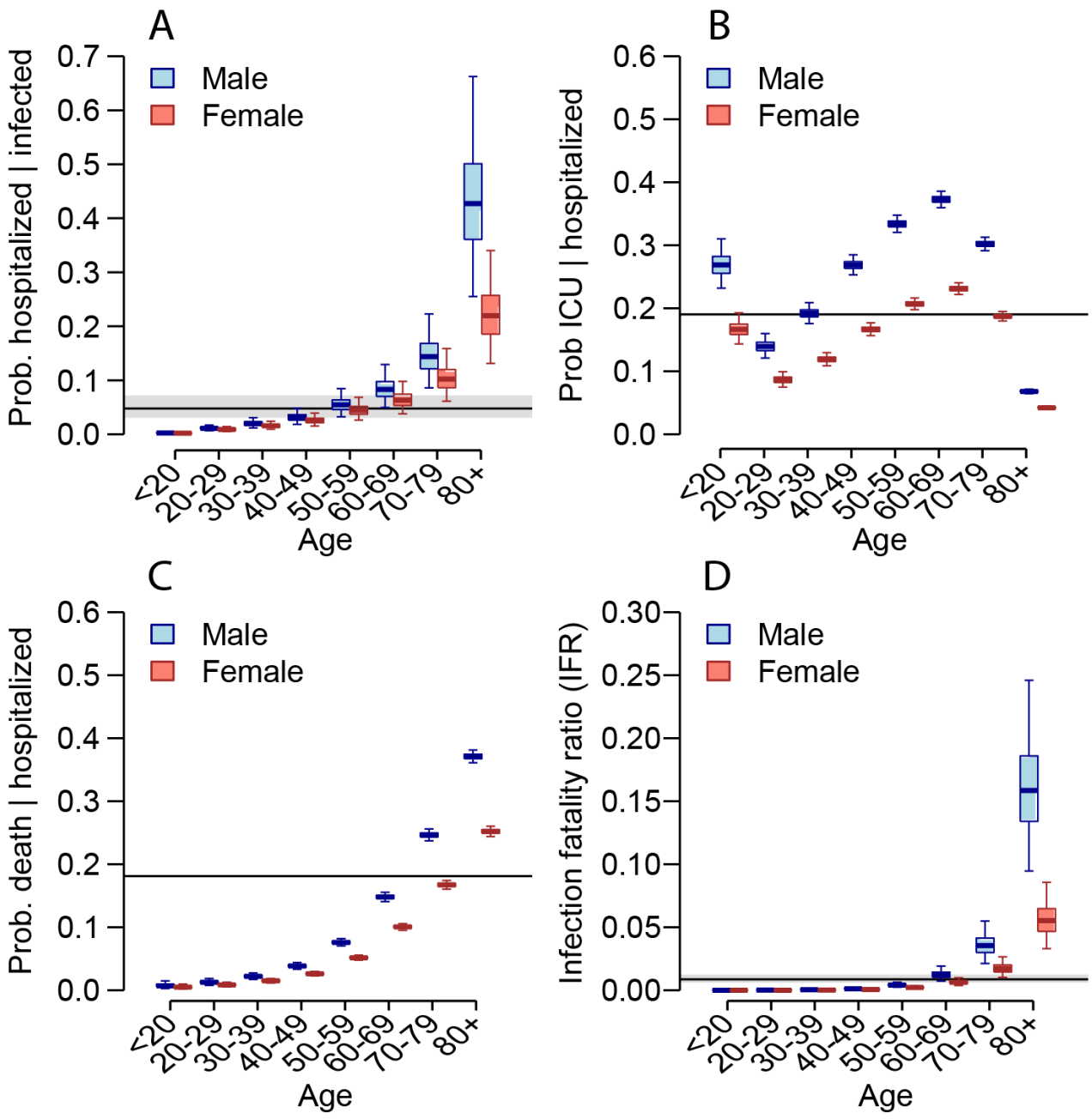

Figure S12: (A) Probability of hospitalization among those infected as a function of age and sex. **(B)** Probability of ICU admission among those hospitalized as a function of age and sex. **(C)** Probability of death among those hospitalized as a function of age and sex. **(D)** Probability of death among those infected as a function of age and sex. For each panel, the black line and grey shaded region represents the overall mean across all ages.

Figure S13: Sensitivity analysis with higher attack rate on Diamond Princess

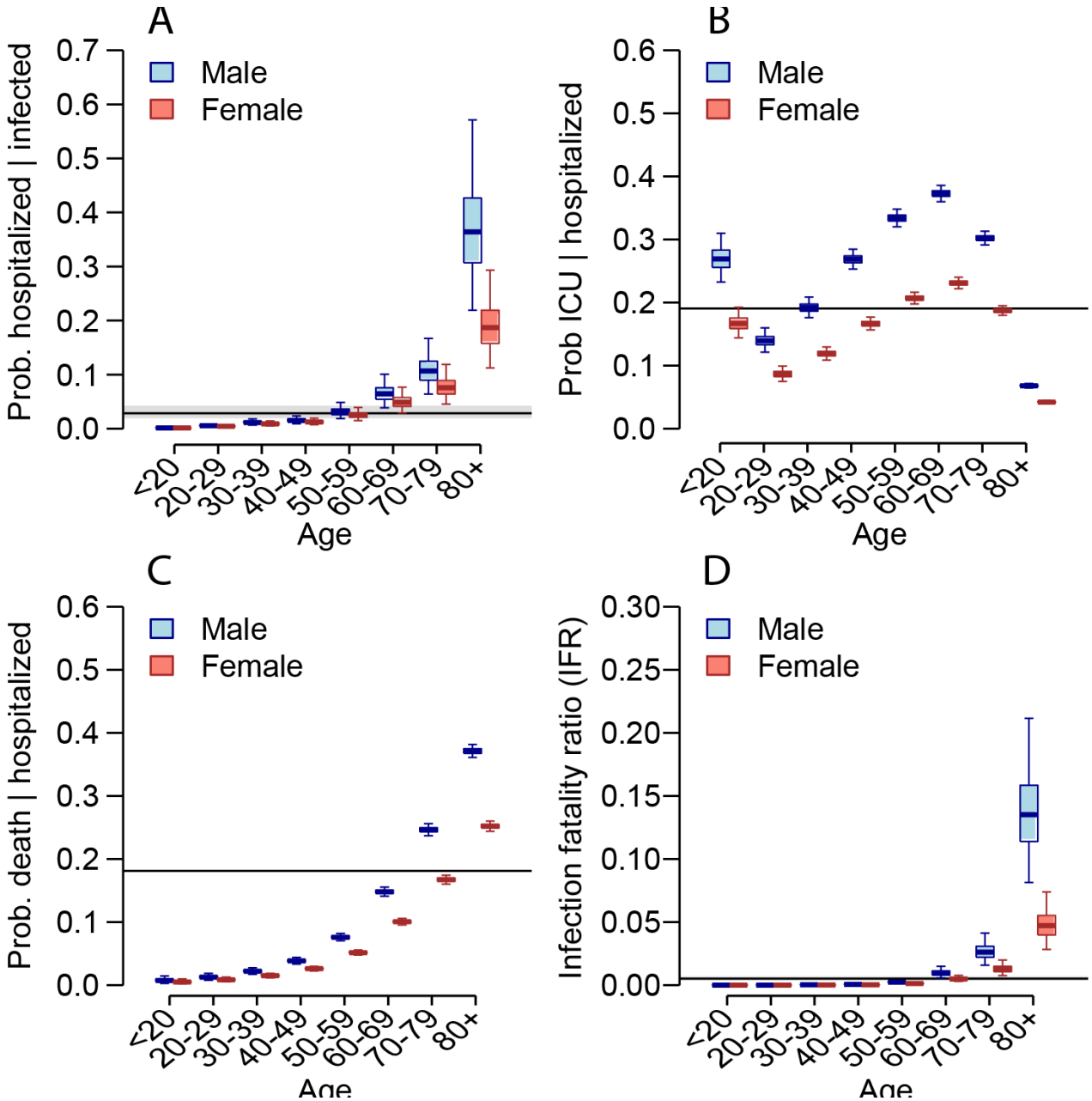

Figure S13: (A) Probability of hospitalization among those infected as a function of age and sex. **(B)** Probability of ICU admission among those hospitalized as a function of age and sex. **(C)** Probability of death among those hospitalized as a function of age and sex. **(D)** Probability of death among those infected as a function of age and sex. For each panel, the black line and grey shaded region represents the overall mean across all ages

Figure S14: Sensitivity analysis with single delay distribution from hospitalization to death

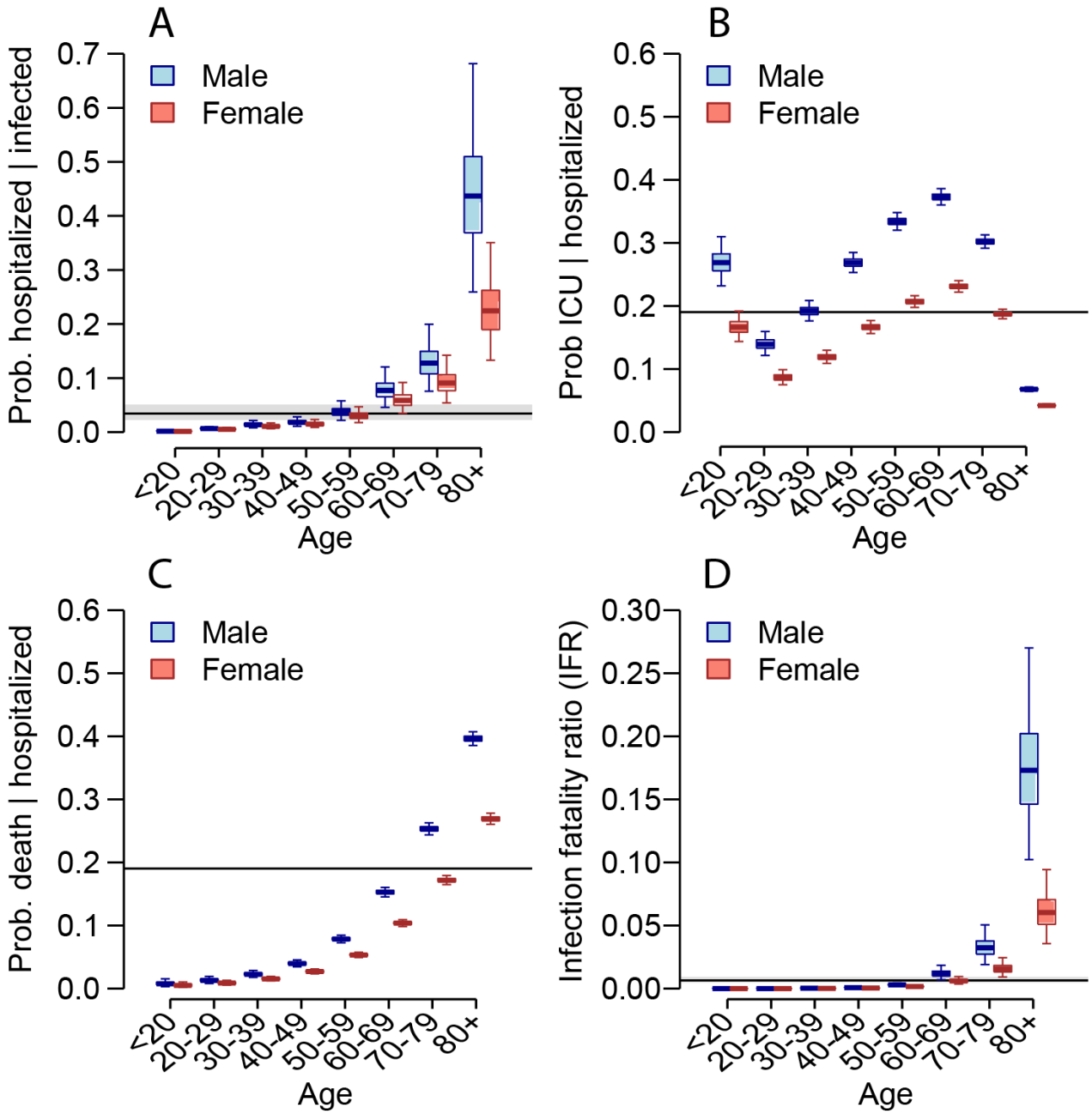

Figure S14: (A) Probability of hospitalization among those infected as a function of age and sex. **(B)** Probability of ICU admission among those hospitalized as a function of age and sex. **(C)** Probability of death among those hospitalized as a function of age and sex. **(D)** Probability of death among those infected as a function of age and sex. For each panel, the black line and grey shaded region represents the overall mean across all ages.

Figure S15 : Time-series of hospitalizations, ICU admissions and deaths corrected for reporting delays

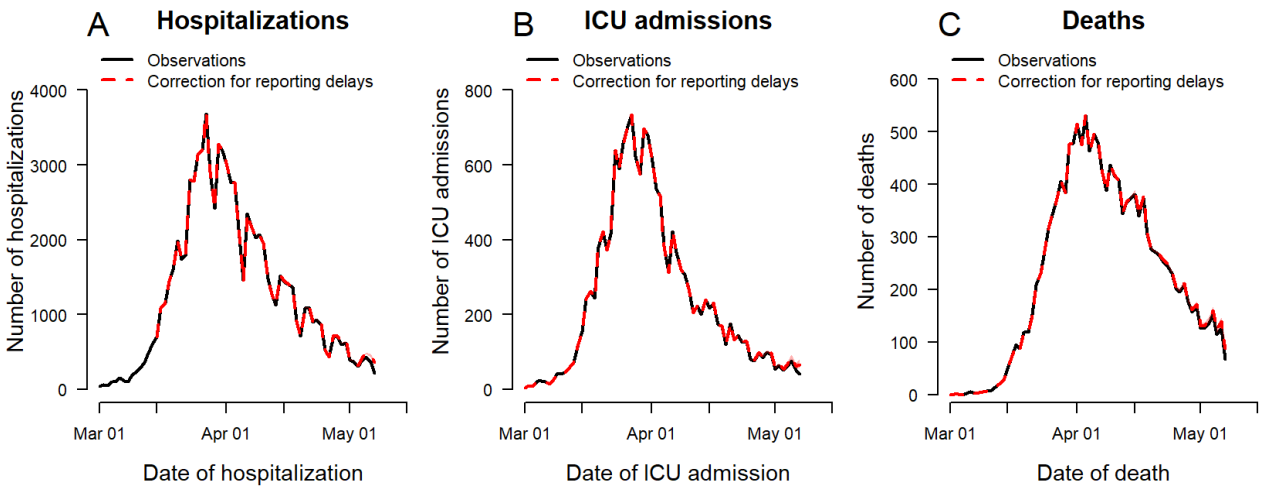

Figure S15: Times-series of hospitalizations (in general ward beds or ICU) **(A)**, ICU admissions **(B)** and deaths **(C)** from SI-VIC data, corrected for reporting delays. See methods section on how the time-series were corrected. Note that the definition of hospitalizations differs from the one used by Santé Publique France. See the Case data section in the methods description for further details.

Figure S16 : **Attack rate per age-group by average number of contacts per day**

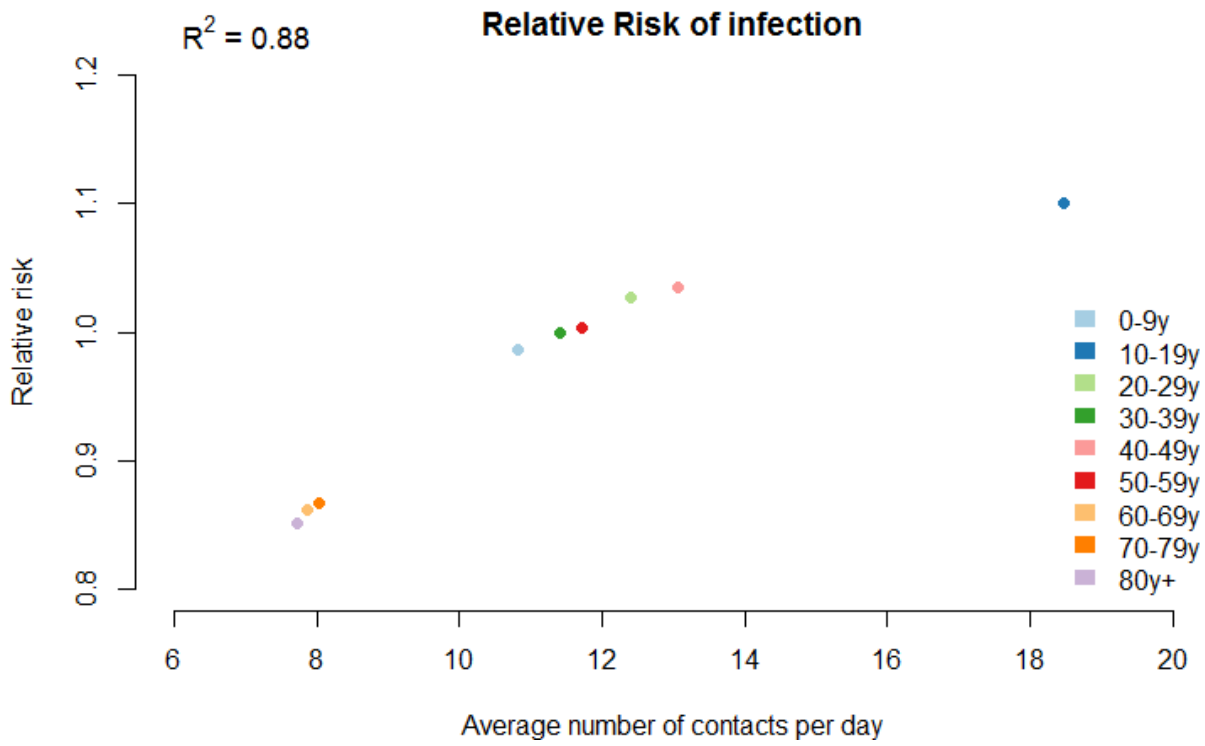

Figure S16: An epidemic is simulated in the French population using an age-structured contact matrix from Béraud et al.(*19*). We use the same parameters for the natural history of the disease as the one used in the main transmission model in the paper. The graph sets out the resulting relative risk of infection per age-group at the end of the epidemic as a function of the average number of contacts per day for a given age-group. The reference age-group is the 30-39 age-group.

Figure S17 : Proportion of ICU admission among hospitalized patients over time

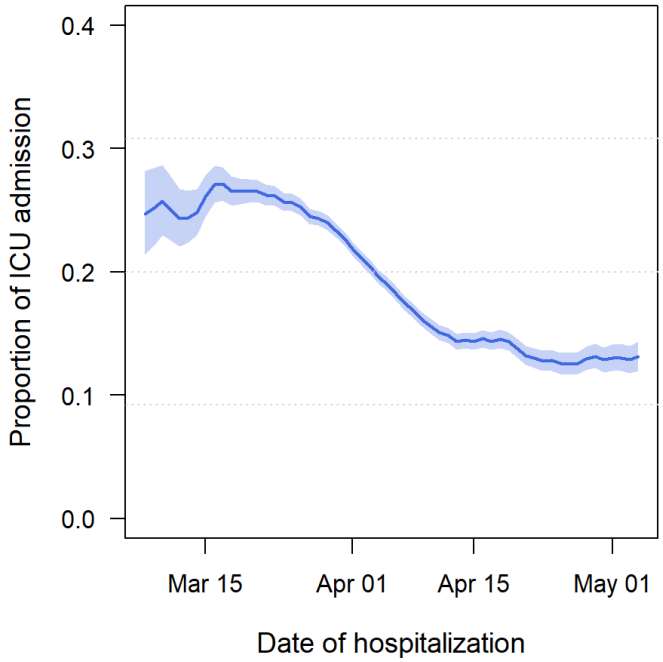

Figure S17: Proportion of ICU admission among hospitalized patients over time (SI-VIC data). We used a 7-day moving window and binomial confidence interval.

Table S1:

Age group	Percent infections hospitalized			Percent of hospitalized cases that go to ICU		
	Male	Female	Mean	Male	Female	Mean
<20	0.2 (0.1-0.3)	0.2 (0.1-0.3)	0.2 (0.1-0.3)	26.9(23.2-31.0)	16.7 (14.4-19.2)	22.2 (19.2-25.5)
20-29	0.7 (0.4- 1.1)	0.6 (0.3-0.9)	0.6 (0.4-1.0)	14.0 (12.2-15.9)	8.6 (7.5-9.9)	11.5 (10.1-13.2)
30-39	1.4 (0.9-2.2)	1.1 (0.7-1.8)	1.3 (0.8-2.0)	19.2 (17.6-20.9)	11.9 (10.9-13.0)	15.9 (14.6-17.3)
40-49	1.9 (1.1-3.0)	1.6 (0.9-2.4)	1.7 (1.0-2.7)	26.9 (25.3-28.5)	16.6 (15.6-17.7)	22.2 (21.0-23.5)
50-59	3.9 (2.3-6.1)	3.2 (1.9-4.9)	3.5 (2.1-5.4)	33.4 (32.0-34.8)	20.7 (19.8-21.7)	27.6 (26.5-28.7)
60-69	8.1 (4.8-12.6)	6.2 (3.7-9.6)	7.1 (4.2-11.0)	37.3 (36.0-38.6)	23.1 (22.2-24.0)	30.8 (29.8-31.8)
70-79	13.4 (8.0-20.7)	9.6 (5.7-14.8)	11.3 (6.7-17.5)	30.2 (29.2-31.3)	18.7 (18.0-19.5)	24.9 (24.1-25.8)
80+	45.9 (27.3-70.9)	23.6 (14.0-36.4)	32.0 (19.0-49.4)	6.8 (6.5-7.2)	4.2 (4.0-4.5)	5.6 (5.3-5.9)
Mean	4.0 (2.4-6.2)	3.2 (1.9-5.0)	3.6 (2.1-5.6)	23.1 (22.6-23.6)	14.3 (13.9-14.7)	19.0 (18.7-19.44)

Table S1: Percent of infections that are hospitalized and end up in ICU by age and sex.
Percentage of infections that are hospitalized and the percentage that end up in ICU, conditional on being hospitalized.

Table S2

Age group	Percent death among those hospitalized			Infection fatality ratio (%)		
	Male	Female	Mean	Male	Female	Mean
<20	0.7 (0.3-1.5)	0.5 (0.2-1.1)	0.6 (0.3-1.3)	0.001 (<0.001-0.003)	0.001 (<0.001-0.002)	0.001 (<0.001-0.002)
20-29	1.3 (0.8-1.9)	0.9 (0.5-1.3)	1.1 (0.7-1.6)	0.008 (0.004-0.02)	0.005 (0.002-0.009)	0.007 (0.003-0.01)
30-39	2.2 (1.7-2.7)	1.5 (1.2-1.9)	1.9 (1.5-2.3)	0.03 (0.02-0.05)	0.02 (0.01-0.03)	0.02 (0.01-0.04)
40-49	3.8 (3.4-4.4)	2.6 (2.3-3.0)	3.3 (2.9-3.7)	0.07 (0.04-0.1)	0.04 (0.02-0.07)	0.06 (0.03-0.09)
50-59	7.6 (7.0-8.2)	5.2 (4.8-5.6)	6.5 (6.0-7.0)	0.3 (0.2-0.5)	0.2 (0.1-0.3)	0.2 (0.1-0.36)
60-69	14.8 (14.1-15.6)	10.1 (9.5-10.6)	12.6 (12.0-13.2)	1.2 (0.7-1.9)	0.6 (0.4-1.0)	0.9 (0.5-1.4)
70-79	24.6 (23.7-25.6)	16.7 (16.0-17.4)	21.0 (20.3-21.8)	3.3 (2.0-5.1)	1.6 (1.0-2.5)	2.4 (1.4-3.7)
80+	37.1 (36.1-38.2)	25.2 (24.4-26.0)	31.6 (30.9-32.4)	17.1 (10.1-26.3)	5.9 (3.5-9.2)	10.1 (6.0-15.6)
Mean	21.22 (20.8-21.7)	14.4 (14.0-14.9)	18..1 (17.8-18.4)	0.8 (0.5-1.3)	0.5 (0.3-0.7)	0.7 (0.4-1.0)

Table S2: Infection fatality. Percent of deaths among those hospitalized and among those infected by age and sex.

Table S3

Age group	Proportion of short delays	Exponential (for short delay)	Lognormal (for longer delays)		Overall Mean (days)
		Mean	Mea (mean for parameterization)	Median (median for parameterization)	
<70	0.11	0.67	15.5 (21.2)	11.4 (12.4)	13.9
70-80	0.13		11.6 (12.6)	8.4 (8.5)	10.2
80+	0.18		10.1 (10.5)	7.4 (7.5)	8.4
Mean	0.15	0.67	11.6	8.5	10.0

Table S3: Estimated delays from hospitalization to death, by age. Means and medians are given in days. For the lognormal distributions, means and medians are corrected accounting for a truncation of 60 days, in brackets are shown values for parameterization.

Table S4: Parameter estimates from the national model

Parameter	**Estimate with 95% credible interval**
Basic reproduction number R_0	2.9 [2.8 - 2.99]
Reproduction number after lockdown $R_{lockdown}$	0.67 [0.65 - 0.68]
Overdispersion parameter δ	0.57 [0.54 - 0.6]
Initial number of cases I_0	48.8 [34.3 - 73.92]
Mean time spent in ICU $2/{g_{ICU}}^{out}$	17.57 [16.97 - 18.2]
Mean time spent in general ward beds $2/{g_{hosp}}^{out}$	13.11 [12.66 - 13.61]
Change in the probability of ICU admission α	0.53 [0.49 - 0.57]

Table S5: Parameter estimates from the regional model

Parameters common to all the regions

Basic reproduction number R_0	2.94 [2.9 - 2.99]
Overdispersion parameter δ	0.69 [0.68 - 0.71]
Reproduction number after lockdown $R_{lockdown}$	0.68 [0.67 - 0.68]
Change in the probability of ICU admission α	0.53 [0.51 - 0.55]

Region specific parameters

ARA: Auvergne-Rhône Alpes *; BFC :* Bourgogne-Franche-Comté ; BRE : Bretagne ; CVL : Centre-Val de Loire ; COR : Corse ; GES : Grand-Est ; HDF : Hauts-de-France ; IDF : Île-de-France ; NAQ : Nouvelle-Aquitaine ; NOR : Normandie ; OCC : Occitanie ; PAC : Provence-Alpes Côte d'Azur ; PDL : Pays de la Loire

Region reg	**Mean time spent in ICU** $2/g_{ICU\,reg}{}^{out}$	**Mean time spent in general ward beds** $2/g_{hosp}{}^{out}$	**Initial number of cases** $I_0{}^{reg}$
ARA	16.98 [16.25 - 17.81]	13 [12.46 - 13.49]	3.96 [3.23 - 4.82]
BFC	16.15 [15.17 - 17.12]	11.61 [11.04 - 12.25]	1.83 [1.47 - 2.24]
BRE	9.91 [8.95 - 10.98]	10.8 [9.94 - 11.72]	0.59 [0.48 - 0.72]
CVL	20.95 [19.3 - 22.8]	17.33 [16.19 - 18.65]	0.85 [0.69 - 1.03]
COR	14.29 [12.28 - 17]	7.79 [6.74 - 8.92]	0.15 [0.12 - 0.19]
GES	14.09 [13.59 - 14.61]	11.86 [11.49 - 12.25]	7.87 [6.38 - 9.56]
HDF	16.91 [16.11 - 17.79]	13.63 [13 - 14.25]	3.55 [2.86 - 4.31]
IDF	20.46 [19.88 - 21.1]	14.94 [14.55 - 15.32]	18.56 [15.12 - 22.47]
NAQ	15.21 [13.99 - 16.51]	11.67 [10.83 - 12.56]	0.89 [0.73 - 1.09]
NOR	17.17 [15.8 - 18.64]	12.58 [11.71 - 13.51]	0.84 [0.67 - 1.02]
OCC	15.63 [14.64 - 16.7]	8.02 [7.55 - 8.5]	1.53 [1.24 - 1.89]
PAC	18.1 [17.09 - 19.25]	12.89 [12.23 - 13.54]	2.08 [1.7 - 2.55]
PDL	12.56 [11.59 - 13.63]	12.43 [11.61 - 13.32]	0.9 [0.73 - 1.1]

Table S6: Proportion infected by region by the 11th May.

Region	**Proportion infected (%)** [with 95% uncertainty range stemming from the uncertainty in the probability of hospitalization following infection]
Auvergne-Rhône Alpes	3.6 [2.3 - 6]
Bourgogne-Franche-Comté	4.5 [2.9 - 7.6]
Bretagne	1.3 [0.8 - 2.3]
Centre-Val de Loire	2.4 [1.6 - 4.1]
Corse	3.1 [2 - 5.3]
Grand-Est	9.1 [6 - 14.6]
Hauts-de-France	4.3 [2.8 - 7.2]
Île-de-France	9.9 [6.6 - 15.7]
Nouvelle-Aquitaine	1.1 [0.7 - 1.9]
Normandie	1.9 [1.2 - 3.2]
Occitanie	1.9 [1.2 - 3.3]
Provence-Alpes Côte d'Azur	2.9 [1.9 - 5]
Pays de la Loire	1.8 [1.1 - 3.1]

Table S7. Percent risk of hospitalization given infection sensitivity analyses

Age	No change in CM	Additional social distance in elderly	Children less infectious	Constant attack rate	25% missed infections on Diamond Princess	Single hosp-death delay distribution	Diamond Princess passengers healthier than French population
<20	0.1 (0.08-0.2)	0.2 (0.09-0.2)	0.2 (0.1-0.4)	0.2 (0.1-0.3)	0.1 (0.08-0.2)	0.2 (0.1-0.3)	0.2 (0.1-0.4)
20-29	0.6 (0.4-1.0)	0.6 (0.3-0.9)	0.7 (0.4-1.0)	1.0 (0.6-1.6)	0.5 (0.3-0.8)	0.6 (0.4-0.9)	0.8 (0.5-1.3)
30-39	1.2 (0.7-1.9)	1.2 (0.7-1.8)	1.3 (0.8-2.1)	1.8 (1.1-2.7)	1.0 (0.6-1.6)	1.2 (0.7-1.9)	1.7 (1.0-2.7)
40-49	1.7 (1.0-2.7)	1.6 (0.9-2.4)	1.8 (1.1-2.7)	2.8 (1.7-4.4)	1.4 (0.8-2.2)	1.7 (1.0-2.6)	2.3 (1.4-3.6)
50-59	3.3 (2.0-5.2)	3.2 (1.9-5.0)	3.5 (2.1-5.4)	4.9 (2.9- 7.6)	2.8 (1.7-4.4)	3.4 (2.0-5.2)	4.7(2.8-7.3)
60-69	7.3 (4.3-11.3)	6.5 (3.8-10.0)	7.1 (4.3-11.1)	7.3 (4.3-11.3)	5.6 (3.4-8.8)	6.8 (4.0-10.6)	9.5 (5.6-14.7)
70-79	11.9 (7.1-18.6)	11.5 (6.8-17.8)	11.1 (6.6-17.2)	12.11 (7.3-18.8)	9.0 (5.4-14.1)	10.8 (6.4-16.8)	15.1 (9.0-23.4)
80+	30.4 (18.0-47.4)	32.2 (18.9-49.9)	32.3 (19.3-50.0)	29.8 (17.8-46.2)	25.4 (15.3-39.8)	30.4 (18.0-47.5)	42.7 (25.4-66.2)
Mean	3.3 (2.0-5.2)	3.3 (1.9-5.1)	3.9 (2.3-6.0)	4.8 (2.9-7.4)	2.9 (1.7-4.5)	3.4 (2.0-5.3)	4.8 (2.9-7.5)

Note that the definition of hospitalizations differs from the one used by Santé Publique France. See the Case data section in the methods description for further details.

Table S8. Percent risk of ICU given hospitalization sensitivity analyses

Age	No change in CM	Additional social distance in elderly	Children less infectious	Constant attack rate	25% missed infections on Diamond Princess	Single hosp-death delay distribution	Diamond Princess passengers healthier than French population
<20	22.2 (19.2-25.6)	22.2 (19.2-25.7)	22.2 (19.2-25.6)	22.2 (19.2-25.6)	22.2(19.2-25.5)	22.2 (19.2-25.6)	22.2 (19.2-225.6)
20-29	11.5 (10.1-13.2)	11.6 (10.0-13.2)	11.6 (10.0-13.2)	11.5 (10.0-13.2)	11.5 (10.0-13.2)	11.6 (10.1-13.2)	11.6 (10.0-13.2)
30-39	15.9 (14.6-17.2)	15.9 (14.6-17.3)	15.9 (14.5-17.3)	15.9 (14.6-17.3)	15.9 (14.6-17.2)	15.9 (14.6-17.2)	15.9 (14.6-17.2)
40-49	22.2 (21.0-23.5)	22.2 (21.0-23.5)	22.2 (21.0-23.5)	22.2 (21.0-23.5)	22.2 (20.9-23.5)	22.2 (20.9-23.5)	22.2 (20.9-23.5)
50-59	27.6 (26.5-28.7)	27.6 (26.5-28.7)	27.6 (26.5-28.7)	27.6 (26.5-28.7)	27.6 (26.5-28.7)	27.6 (26.5-28.7)	27.6 (26.5-28.7)
60-69	30.8 (29.8-31.8)	30.8 (29.8-31.8)	30.8 (29.8-31.8)	30.8 (29.8-31.8)	30.8 (29.8-31.8)	30.8 (29.8-31.8)	30.8 (29.8-31.8)
70-79	24.9 (24.1-25.8)	24.9 (24.1-25.8)	24..9 (24.1-25.8)	24.9 (24.1-25.8)	24.9 (24.1-25.8)	24.9 (24.1-25.8)	24.9 (24.1-25.8)
80+	5.6 (5.3 5.9)	5.6 (5.3 5.9)	5.6 (5.3 5.9)	5.6 (5.3 5.9)	5.6 (5.3 5.9)	5.6 (5.3 5.9)	5.6 (5.3 5.9)
Mean	19.1 (18.7-19.3)	19.0 (18.7-19.4)	19.0 (18.7-19.4)	19.0 (18.7-19.4)	19.0 (18.7-19.4)	19.0 (18.7-19.4)	19.2 (18.7-19.4)

Table S9. Percent risk of death given hospitalization sensitivity analyses

Age	No change in CM	Additional social distance in elderly	Children less infectious	Constant attack rate	25% missed infections on Diamond Princess	Single hosp-death delay distribution	Diamond Princess passengers healthier than French population
<20	0.6 (0.2-1.2)	0.6 (0.2-1.3)	0.6 (0.2-1.3)	0.6 (0.2-1.3)	0.6 (0.3-1.2)	0.6 (0.3-1.3)	0.6 (0.2-1.3)
20-29	1.1 (0.7-1.6)	1.1 (0.7-1.6)	1.1 (0.7-1.6)	1.1 (0.7-1.6)	1.1 (0.7-1.6)	1.1 (0.7-1.7)	1.1 (0.7-1.6)
30-39	1.9 (1.5-2.4)	1.9 (1.5-2.3)	1.9 (1.5-2.3)	1.9 (1.5-2.3)	1.9 (1.5-2.4)	1.9 (1.5-2.4)	1.9 (1.5-2.3)
40-49	3.3 (2.9-3.7)	3.3 (2.8-3.7)	3.3 (2.8-3.8)	3.3 (2.9-3.8)	3.3 (2.9-3.7)	3.4 (2.9-3.9)	3.3 (2.9-3.8)
50-59	6.5 (6.0-7.0)	6.5 (6.0-7.0)	6.5 (6.0-7.0)	6.5 (6.0-7.0)	6.5 (6.0-7.0)	6.7 (6.2-7.2)	6.5 (6.0-7.0)
60-69	12.6 (12.0-13.2)	12.6 (12.0-13.2)	12.6 (12.0-13.2)	12.6 (12.0-13.2)	12.6 (12.0-13.2)	13.0 (12.4-13.7)	12.6 (12.0-13.2)
70-79	21.0 (20.3-21.8)	21.0 (20.3-21.8)	21.0 (20.2-21.88)	21.0 (20.3-21.8)	21.0 (20.3-21.8)	21.6 (20.8-22.4)	21.0 (20.3-21.8)
80+	31.6 (30.9-32.4)	31.6 (30.9-32.4)	31.6 (30.9-32.4)	31.6 (30.9-32.4)	31.6 (30.9-32.4)	33.8 (33.0-34.6)	31.6 (30.9-32.4)
Mean	18.1 (17.8-18.4)	18.1 (17.8-18.4)	18.1 (17.8-18.4)	18.1 (17.8-18.4)	18.1 (17.8-18.4)	19.0 (18.7-19.4)	18.1 (17.8-18.4)

Table S10. Percent risk of death given infection (IFR) sensitivity analyses

Age	No change in CM	Additional social distance in elderly	Children less infectious	Constant attack rate	25% missed infections on Diamond Princess	Single hosp-death delay distribution	Diamond Princess passengers healthier than French population
<20	0.001 (<0.001-0.002)	0.001 (<0.001-0.002)	0.001 (<0.001-0.003)	0.001 (<0.001-0.003)	0.001 (<0.001-0.002)	0.001 (<0.001-0.002)	0.001 (0.001-0.003)
20-29	0.007 (0.003-0.01)	0.006 (0.003-0.01)	0.007 (0.004-0.01)	0.01 (0.005-0.02)	0.005 (0.003-0.01)	0.007 (0.003-0.01)	0.009 (0.004-0.02)
30-39	0.02 (0.01-0.04)	0.02 (0.01-0.04)	0.03 (0.01-0.04)	0.03 (0.02-0.05)	0.02 (0.01-0.03)	0.02 (0.01-0.04)	0.03 (0.02-0.05)
40-49	0.06 (0.03-0.09)	0.05 (0.03-0.08)	0.06 (0.03-0.09)	0.09 (0.05-0.1)	0.05 (0.03-0.07)	0.06 (0.03-0.09)	0.08 (0.04-0.1)
50-59	0.2 (0.1-0.3)	0.2 (0.1-0.3)	0.2 (0.1-0.4)	0.3 (0.2-0.5)	0.2 (0.1-0.3)	0.2 (0.1-0.4)	0.3 (0.2-0.5)
60-69	0.9 (0.5-1.4)	0.8 (0.5-1.3)	0.9 (0.5-1.4)	0.9 (0.5-1.4)	0.7 (0.4-1.1)	0.9 (0.5-1.4)	1.2 (0.7-1.9)
70-79	2.5 (1.5-3.9)	2.4 (1.4-3.7)	2.3 (1.4-3.6)	2.5 (1.5-3.9)	1.9 (1.1-3.0)	2.3 (1.4-3.6)	3.2 (1.9-4.9)
80+	9.6 (5.7-15.0)	10.2 (6.0-15.8)	10.2 (6.1-15.8)	9.4 (5.6-14.6)	8.0 (4.8-12.6)	10.3 (6.1-16.1)	13.5 (8.0-20.9)
Mean	0.6 (0.4-0.9)	0.6 (0.4-0.9)	0.7 (0.4-1.1)	0.9 (0.5-1.3)	0.5 (0.3-0.8)	0.7 (0.4-1.0)	0.9 (0.5-1.3)

Table S11. Deviance information criterion (DIC) for the different sensitivity analyses

Sensitivity analysis scenario	**DIC**
Baseline CL_1after the lockdown	2971.12
Children less infectious CL_2after the lockdown	2972.34
No Change CM CL_3after the lockdown	2971.21
CM with SDE CL_4after the lockdown	2970.19
Constant Attack Rates CL_5after the lockdown	2974.80
Increased IFR on Princess Diamond	2972.28
Higher AR Diamond Princess	2970.20
Use single delay distribution from hospitalization to death	2970.37
Longer delay to hospitalization	2989.17

Table S12. Sensitivity analyses - Predictions by May 11th

	Daily new infections	Proportion infected
Baseline	3920 [2580 - 6340]	4.4 [2.8 - 7.2]
Children less inf	4650 [3030 - 7450]	3.5 [2.2 - 5.8]
No Change CM	6510 [4530 - 9630]	5.3 [3.4 - 8.6]
CM SDE	4990 [3310 - 8040]	4.8 [3.1 - 8]
Constant AR	3830 [2470 - 6350]	2.6 [1.7 - 4.3]
Higher IFR	2980 [1950 - 4800]	3.3 [2.1 - 5.5]
Higher AR DP	4860 [3170 - 7620]	5.5 [3.5 - 8.9]
Delay Distrib	4080 [2650 - 6590]	4.6 [3 - 7.6]
Higher delay to hosp	2510 [1660 - 4010]	4.4 [2.9 - 7.4]

References

1. M. U. G. Kraemer, C.-H. Yang, B. Gutierrez, C.-H. Wu, B. Klein, D. M. Pigott, Open COVID-19 Data Working Group, L. du Plessis, N. R. Faria, R. Li, W. P. Hanage, J. S. Brownstein, M. Layan, A. Vespignani, H. Tian, C. Dye, O. G. Pybus, S. V. Scarpino, The effect of human mobility and control measures on the COVID-19 epidemic in China. *Science* (2020), doi:10.1126/science.abb4218.

2. H. Tian, Y. Liu, Y. Li, C.-H. Wu, B. Chen, M. U. G. Kraemer, B. Li, J. Cai, B. Xu, Q. Yang, B. Wang, P. Yang, Y. Cui, Y. Song, P. Zheng, Q. Wang, O. N. Bjornstad, R. Yang, B. T. Grenfell, O. G. Pybus, C. Dye, An investigation of transmission control measures during the first 50 days of the COVID-19 epidemic in China. *Science* (2020), doi:10.1126/science.abb6105.

3. J. Lourenço, R. Paton, M. Ghafari, M. Kraemer, C. Thompson, P. Simmonds, P. Klenerman, S. Gupta, Fundamental principles of epidemic spread highlight the immediate need for large-scale serological surveys to assess the stage of the SARS-CoV-2 epidemic. *medRxiv* (2020) (available at https://www.medrxiv.org/content/10.1101/2020.03.24.20042291v1.abstract).

4. L. Bao, W. Deng, H. Gao, C. Xiao, J. Liu, J. Xue, Q. Lv, J. Liu, P. Yu, Y. Xu, F. Qi, Y. Qu, F. Li, Z. Xiang, H. Yu, S. Gong, M. Liu, G. Wang, S. Wang, Z. Song, W. Zhao, Y. Han, L. Zhao, X. Liu, Q. Wei, C. Qin, Reinfection could not occur in SARS-CoV-2 infected rhesus macaques. *bioRxiv*, , doi:10.1101/2020.03.13.990226.

5. J. Lessler, H. Salje, M. D. Van Kerkhove, N. M. Ferguson, S. Cauchemez, I. Rodriquez-Barraquer, R. Hakeem, T. Jombart, R. Aguas, A. Al-Barrak, D. A. T. Cummings, MERS-CoV Scenario and Modeling Working Group, Estimating the Severity and Subclinical Burden of Middle East Respiratory Syndrome Coronavirus Infection in the Kingdom of Saudi Arabia. *Am. J. Epidemiol.* **183**, 657–663 (2016).

6. R. Verity, L. C. Okell, I. Dorigatti, P. Winskill, C. Whittaker, N. Imai, G. Cuomo-Dannenburg, H. Thompson, P. G. T. Walker, H. Fu, A. Dighe, J. T. Griffin, M. Baguelin, S. Bhatia, A. Boonyasiri, A. Cori, Z. Cucunubá, R. FitzJohn, K. Gaythorpe, W. Green, A. Hamlet, W. Hinsley, D. Laydon, G. Nedjati-Gilani, S. Riley, S. van Elsland, E. Volz, H. Wang, Y. Wang, X. Xi, C. A. Donnelly, A. C. Ghani, N. M. Ferguson, Estimates of the severity of coronavirus disease 2019: a model-based analysis. *Lancet Infect. Dis.* (2020), doi:10.1016/S1473-3099(20)30243-7.

7. T. W. Russell, J. Hellewell, C. I. Jarvis, K. van Zandvoort, S. Abbott, R. Ratnayake, Cmmid Covid-Working Group, S. Flasche, R. M. Eggo, W. J. Edmunds, A. J. Kucharski, Estimating the infection and case fatality ratio for coronavirus disease (COVID-19) using age-adjusted data from the outbreak on the Diamond Princess cruise ship, February 2020. *Euro Surveill.* **25** (2020), doi:10.2807/1560-7917.ES.2020.25.12.2000256.

8. K. Mizumoto, K. Kagaya, G. Chowell, Early epidemiological assessment of the transmission potential and virulence of coronavirus disease 2019 (COVID-19) in Wuhan City: China, January-February, 2020. *medRxiv* (2020) (available at https://www.medrxiv.org/content/10.1101/2020.02.12.20022434v2.abstract).

9. L. Peeples, News Feature: Avoiding pitfalls in the pursuit of a COVID-19 vaccine. *Proc. Natl. Acad. Sci. U. S. A.* (2020), doi:10.1073/pnas.2005456117.

10. D. Ricke, R. W. Malone, Medical Countermeasures Analysis of 2019-nCoV and Vaccine Risks for Antibody-Dependent Enhancement (ADE) (2020), , doi:10.2139/ssrn.3546070.

11. J. Yang, Y. Zheng, X. Gou, K. Pu, Z. Chen, Q. Guo, R. Ji, H. Wang, Y. Wang, Y. Zhou, Prevalence of comorbidities and its effects in patients infected with SARS-CoV-2: a systematic review and meta-analysis. *International Journal of Infectious Diseases*. **94** (2020), pp. 91–95.

12. M. Bolles, D. Deming, K. Long, S. Agnihothram, A. Whitmore, M. Ferris, W. Funkhouser, L. Gralinski, A. Totura, M. Heise, R. S. Baric, A Double-Inactivated Severe Acute Respiratory Syndrome Coronavirus Vaccine Provides Incomplete Protection in Mice and Induces Increased Eosinophilic Proinflammatory Pulmonary Response upon Challenge. *Journal of Virology*. **85** (2011), pp. 12201–12215.

13. A. Fontanet, L. Tondeur, Y. Madec, R. Grant, C. Besombes, N. Jolly, S. F. Pellerin, M.-N. Ungeheuer, I. Cailleau, L. Kuhmel, Others, Cluster of COVID-19 in northern France: A retrospective closed cohort study. *medRxiv* (2020) (available at https://www.medrxiv.org/content/10.1101/2020.04.18.20071134v1.abstract).

14. L. Grzelak, S. Temmam, C. Planchais, C. Demeret, SARS-CoV-2 serological analysis of COVID-19 hospitalized patients, pauci-symptomatic individuals and blood donors. *medRxiv* (2020) (available at https://www.medrxiv.org/content/10.1101/2020.04.21.20068858v1?rss=1).

15. info coronavirus covid 19 - carte et donnees covid 19 en france. *Gouvernement.fr*, (available at https://www.gouvernement.fr/info-coronavirus/carte-et-donnees).

16. Field Briefing: Diamond Princess COVID-19 Cases, 20 Feb Update (2020), (available at https://www.niid.go.jp/niid/en/2019-ncov-e/9417-covid-dp-fe-02.html).

17. 新型コロナウイルス感染症について (About new coronavirus infection), (available at https://www.mhlw.go.jp/stf/seisakunitsuite/bunya/0000164708_00001.html).

18. H. Nishiura, D. Klinkenberg, M. Roberts, J. A. P. Heesterbeek, Early epidemiological assessment of the virulence of emerging infectious diseases: a case study of an influenza pandemic. *PLoS One*. **4**, e6852 (2009).

19. G. Béraud, S. Kazmercziak, P. Beutels, D. Levy-Bruhl, X. Lenne, N. Mielcarek, Y. Yazdanpanah, P.-Y. Boëlle, N. Hens, B. Dervaux, The French Connection: The First Large Population-Based Contact Survey in France Relevant for the Spread of Infectious Diseases. *PLoS One*. **10**, e0133203 (2015).

20. K. Mizumoto, K. Kagaya, A. Zarebski, G. Chowell, Estimating the asymptomatic proportion of coronavirus disease 2019 (COVID-19) cases on board the Diamond Princess cruise ship, Yokohama, Japan, 2020. *Euro Surveill.* **25** (2020), doi:10.2807/1560-7917.ES.2020.25.10.2000180.

21. Stan Development Team, RStan: the R interface to Stan (2020), (available at http://mc-stan.org/).

22. Zhanwei Du, Xiaoke Xu, Ye Wu, Lin Wang, Benjamin J. Cowling, Lauren Ancel Meyers, Serial Interval of COVID-19 among Publicly Reported Confirmed Cases. *Emerging*

Infectious Disease journal. **26** (2020), doi:10.3201/eid2606.200357.

23. Q. Bi, Y. Wu, S. Mei, C. Ye, X. Zou, Z. Zhang, X. Liu, L. Wei, S. A. Truelove, T. Zhang, W. Gao, C. Cheng, X. Tang, X. Wu, Y. Wu, B. Sun, S. Huang, Y. Sun, J. Zhang, T. Ma, J. Lessler, T. Feng, Epidemiology and Transmission of COVID-19 in Shenzhen China: Analysis of 391 cases and 1,286 of their close contacts. *medRxiv*, 2020.03.03.20028423 (2020).

24. L. Tindale, M. Coombe, J. E. Stockdale, E. Garlock, W. Y. V. Lau, M. Saraswat, Y.-H. B. Lee, L. Zhang, D. Chen, J. Wallinga, C. Colijn, Transmission interval estimates suggest pre-symptomatic spread of COVID-19. *Epidemiology* (2020), , doi:10.1101/2020.03.03.20029983.

25. S. Funk, *socialmixr* (Github; https://github.com/sbfnk/socialmixr).

26. O. Diekmann, J. A. Heesterbeek, J. A. Metz, On the definition and the computation of the basic reproduction ratio R0 in models for infectious diseases in heterogeneous populations. *J. Math. Biol.* **28**, 365–382 (1990).

27. N. Hens, G. M. Ayele, N. Goeyvaerts, M. Aerts, J. Mossong, J. W. Edmunds, P. Beutels, Estimating the impact of school closure on social mixing behaviour and the transmission of close contact infections in eight European countries. *BMC Infect. Dis.* **9**, 187 (2009).

28. Décret n° 2020-260 du 16 mars 2020 portant réglementation des déplacements dans le cadre de la lutte contre la propagation du virus covid-19 | Legifrance, (available at https://www.legifrance.gouv.fr/affichTexte.do?cidTexte=JORFTEXT000041728476&categorieLien=id).

29. A. Gelman, J. B. Carlin, H. S. Stern, D. B. Rubin, Bayesian Data Analysis Chapman & Hall. *CRC Texts in Statistical Science* (2004).

30. COVID-19 Community Mobility Report. *COVID-19 Community Mobility Report*, (available at https://www.google.com/covid19/mobility/).

31. J. Wallinga, M. Lipsitch, How generation intervals shape the relationship between growth rates and reproductive numbers. *Proc. Biol. Sci.* **274**, 599–604 (2007).